The analysis of the Generalized-a method for non-linear dynamic problems

Silvano Erlicher, Luca Bonaventura, Oreste Bursi

The analysis of the $Generalized - \alpha$ methods for non-linear dynamic problems

Silvano Erlicher*
Dipartimento di Ingegneria Meccanica e Strutturale,
Università di Trento, Via Mesiano 77, 38050 Trento, Italy

Luca Bonaventura
Dipartimento di Ingegneria Civile e Ambientale,
Università di Trento, Via Mesiano 77, 38050 Trento, Italy

Oreste S. Bursi
Dipartimento di Ingegneria Meccanica e Strutturale,
Università di Trento, Via Mesiano 77, 38050 Trento, Italy

February 2001

Abstract

This paper presents the consistency and stability analyses of the $Generalized - \alpha$ methods applied to non-linear dynamical systems. The second-order accuracy of this class of algorithms is proved also in the non-linear regime, independently of the quadrature rule for non-linear internal forces. Conversely, the G-stability notion which is suitable for linear multistep schemes devoted to non-linear dynamic problems cannot be applied, as the non-linear structural dynamics equations are not contractive. Nonetheless, it is proved that the $Generalized - \alpha$ methods are endowed with stability in an energy sense and guarantee energy decay in the high-frequency range as well as asymptotic annihilation. However, overshoot and heavy energy oscillations in the intermediate-frequency range are exhibited. The results of representative numerical simulations performed on relatively simple single- and multiple-degrees-of-freedom non-linear systems are presented in order to confirm the analytical estimates.

KEY WORDS: $Generalized - \alpha$ methods; non-linear dynamics; non-linear (energy) stability; energy-decaying schemes; overshoot; algorithmic damping.

*$Correspondence\ to:$ Silvano Erlicher, Dipartimento di Ingegneria Meccanica e Strutturale, Università di Trento, Via Mesiano 77, 38050 Trento, Italy. E-mail: silvano.erlicher@ing.unitn.it

Contents

1   Introduction

For many problems in structural dynamics, the time integration of *stiff* ordinary differential equations is required (Hairer and Wanner (1991), p. 9). Commonly used methods for integrating equations with timescales that differ by several orders of magnitude are implicit as relatively large time steps can be employed. As a matter of fact, most integration schemes are A-stable, i.e. unconditionally stable in the linear regime. Moreover, it is essential that these methods be endowed with mechanisms entailing numerical dissipation in the high-frequency range, with limited algorithmic damping in the low-frequency range. These mechanisms help to eliminate high-frequency modes that are insufficiently resolved by either the spatial discretization, the

selected time step or both. Representative members of these algorithms are, among others, the $N-\beta$ method (Newmark (1959)), the $HHT-\alpha$ method (Hilber, Hughes and Taylor (1977)), the $WBZ-\alpha$ method (Wood, Bossak and Zienkiewicz (1981)), the $HP-\theta_1$ method (Hoff and Pahl (1988a), (1988b)) and the $CH-\alpha$ method (Chung and Hulbert (1993)). These methods exhibit second order accuracy in linear dynamics and permit efficient variable step size techniques, being one-step methods. The $CH-\alpha$, the $HHT-\alpha$ and the $WBZ-\alpha$ methods, the so-called $\alpha-$ methods, are one-parameter schemes which can be considered as particular cases of a more general class of methods named $Generalized-\alpha$ $(G-\alpha)$ in the foregoing. This class of methods corresponds to the $CH-\alpha$ scheme (Chung and Hulbert (1993)), where the algorithmic parameters α_m, α_f, β and γ are assumed to be independent of each other.

For *stiff* linear problems, A-stability may not be sufficient to ensure a robust temporal integration. As a matter of fact, some *stiff* components of the numerical solution damp out very slowly even in the presence of numerical dissipation and can show up oscillations which alter the solution. The low effectiveness of the numerical dissipation and the overshoot consequences on the response of the $HHT-\alpha$ method applied to *stiff* dynamical systems have been highlighted by Bauchau, Damilano and Theron (1995). Recently, Piché (1995) and (Owren (1995) proposed Rosenbrock and Runge-Kutta methods, respectively, with better accuracy and stability properties than those of the Constant Average Acceleration (CAA) scheme (Newmark (1959)). More specifically, these methods are L-stable and do not exhibit overshoot. Moreover, the L-stability property entails A-stability and asymptotic annihilation, viz. these schemes damp out almost in a single time step any non-zero response in the high-frequency modes (Hulbert (1991)). L-stability combined with the optimized dissipation characteristics of higher modes represent the attractive properties in the linear regime of the $CH-\alpha$ method (Chung and Hulbert (1993)). These properties can be user-controlled by means of the spectral radius at infinity $\rho_\infty (= \rho(\Omega)$ for $\Omega \to \infty)$; more specifically $\rho_\infty \in [0,1]$ and the choice $\rho_\infty = 0$ corresponds to the case of asymptotic annihilation of the high-frequency response, while $\rho_\infty = 1$ corresponds to the case of no algorithmic dissipation. The $CH-\alpha$ scheme has already been applied successfully to inertial and wave propagation problems and allows adaptive time-stepping (Hulbert and Jang (1995)). Hulbert and Hughes (1987) proved that the $HHT-\alpha$ scheme suffers from the velocity overshoot

3

and that the acceleration is only first order accurate. Later, it is also proved that the $CH - \alpha$ method and, more in general the class of $G - \alpha$ methods, inherits these unwanted properties.

Time-stepping algorithms often represent the only tool that can be exploited for the analysis of non-linear problems, though a rigorous convergence analysis of such algorithms is feasible only in the linear case. As a matter of fact, algorithms regarded as unconditionally stable in linear dynamics, like the CAA scheme, can exhibit severe numerical instabilities in the non-linear regime. To this regard see, among others, Simo and Tarnow (1992), Wood and Oduor (1988) and Bauchau, Damilano and Theron (1995). Moreover, these methods may converge to spurious solutions associated with a high energy state (Crisfield and Shi (1994)). The numerical stability of time-stepping schemes in non-linear structural dynamics was analysed in some studies. In detail, Park (1975) performed the local stability analysis of the Houbolt method (Houbolt (1950)) and the CAA method. Belytschko and Schoeberle (1975) proved that the CAA scheme complies with an energy convergence criterion which represents a sufficient condition for the non-linear unconditional (energy) stability of the numerical algorithm. Hughes extended the same result to the $N - \beta$ method (Hughes (1975)) . Again, Hughes (1976) performed an analysis of the stability, accuracy and energy properties of the CAA method in the non linear regime.

Due to its favourable properties, the $CH - \alpha$ method augmented with energy and momentum constraints was recently adopted as a basic algorithm for the non linear dynamics analysis of shell structures (Kuhl and Ramm (1996)). Moreover, it represented the algorithmic environment for the development of a new class of algorithms applied to non-linear elasto-dynamics and labelled Generalized Energy-Momentum methods (Kuhl and Crisfield (1999) and Kuhl and Ramm (1998)) . Crisfield and his co-workers, compared the performances of the $\alpha-$ methods with those of energy-conserving algorithms in non-linear elasto-dynamics (Crisfield, Galvanetto and Jelenic (1997) and Zhong and Crisfield (1998)). This research work showed clearly the unfavourable energy-decaying properties of the $\alpha-$ methods. As a matter of fact, this class of methods exhibited overshoot phenomena, energy oscillations and blow-up for large time steps and certain algorithmic parameter values. Recent approaches successfully employed both in linear and non-linear transient/dynamic cases are the Virtual-Pulse time integral method and the generalized W_p-Family of operators, respectively, developed by Tamma and co-workers (2000). In non-linear

dynamics the resulting algorithms exhibit favourable algorithmic and computational properties over standard integration operators.

Though numerous studies have dealt with the $\alpha-$ methods, there is still a paucity of publications devoted to the clarification of specific issues in the non-linear regime, such as accuracy, stability, energy-decaying properties, overshoot, high-frequency behaviour and numerical integration of internal forces. All together, they represents basic aspects of the temporal integration of non linear systems and are the issues that the paper explores further. The remainder of the paper is organized as follows. In Section 2, the class of $G - \alpha$ methods is applied to the non-linear equations of structural dynamics according to a single-step as well as to a linear multistep formulation. Moreover, three alternatives for the temporal integration of non-linear internal forces are presented: the generalized trapezoidal rule, the mid-point rule and the generalized energy-momentum rule. Section 3 presents the consistency analysis of the $G - \alpha$ methods, demonstrating that the second order accuracy of displacements is also maintained in the non-linear regime. Moreover, the conditions under which the acceleration is second order accurate are shown. In Section 4, the contractivity of the equations of structural dynamics and the stability properties of these methods in the non-linear regime are investigated. Section 5 analyses both the overshoot and the high-frequency behaviour of the class of $G - \alpha$ methods as well as the dissipation properties. In Section 6, numerical experiments performed on relatively simple non-linear single- (S.D.o.F.) and multiple-degrees-of-freedom (M.D.o.F.) test problems which legitimate analytical findings are reported, while conclusions are drawn in Section 7. Finally, the properties of the $G - \alpha$ methods relevant to the linear regime are recalled in Appendix 1.

2 The equations of structural dynamics and the $G - \alpha$ methods

The semidiscrete initial value problem for non-linear structural dynamics reads

$$\mathbf{M}\ddot{\mathbf{u}}(t) + \mathbf{C}\dot{\mathbf{u}}(t) + \mathbf{S}\left(\mathbf{u}(t)\right) = \mathbf{F}(t) \tag{1}$$

where $\mathbf{M}$ and $\mathbf{C}$ are the mass and damping matrices, respectively, $\mathbf{S}\left(\mathbf{u}(t)\right)$ is the vector of non-linear internal forces, $\mathbf{F}(t)$ is the vector of applied loads, $\mathbf{u}(t)$ is the displacement vector and superimposed dots indicate time differentiation. The initial value problem consists of determining a function $\mathbf{u} = \mathbf{u}(t)$ which satisfies Eq. (1) for all $t \in [0, t_f]$, $t_f > 0$, with given initial

5

conditions

$$\mathbf{u}(0) = \mathbf{d} , \quad \dot{\mathbf{u}}(0) = \mathbf{v}. \tag{2}$$

$\mathbf{M}$ and $\mathbf{C}$ are assumed to be both constant and symmetric. Moreover, $\mathbf{M}$ is positive definite, $\mathbf{C}$ is positive semidefinite, $\mathbf{F}$ is considered a smooth function of t while $\mathbf{S} = \mathbf{S}(\mathbf{u}(t))$ fulfils the Lipschitz continuity in each time interval. In addition, a positive smooth scalar function $U = U(\mathbf{u}(t))$ exists, the potential energy, such that $\nabla U(\mathbf{u}(t)) = \mathbf{S}(\mathbf{u}(t))$ and $U(\mathbf{0}) = 0$.

With this notation to hand, the class of $G - \alpha$ methods is applied to Eq. (1) and, for analysis purposes, both the single-step and the linear multistep formulation are considered (Hairer, Nørsett and Wanner (1987) p. 304, Hughes (1987), p. 526 and Hulbert (1991)). Moreover, the linearization of Eq. (1) and the iterative solution strategy are described.

2.1 Single-step three-stage formulation

Let $0 = t_0 < t_1 < \ldots < t_m = t_f$ be a partition of the time domain and let $\Delta t_i = t_{i+1} - t_i$ be the time step size. For brevity, a constant Δt value is assumed hereinafter. The $G - \alpha$ methods applied to the Eq. (1) and (2) yield the balance equation

$$\mathbf{M}\mathbf{a}_{i+1-\alpha_m} + \mathbf{C}\mathbf{v}_{i+1-\alpha_f} + \mathbf{S}_{i+1-\alpha_f} = \mathbf{F}_{i+1-\alpha_f} \tag{3}$$

where the dynamic equilibrium is computed at some instant inside Δt_i. Moreover,

$$\mathbf{d}_{i+1} = \mathbf{d}_i + \Delta t \mathbf{v}_i + \Delta t^2 \left(\left(\frac{1}{2} - \beta \right) \mathbf{a}_i + \beta \mathbf{a}_{i+1} \right) \tag{4}$$

$$\mathbf{v}_{i+1} = \mathbf{v}_i + \Delta t \left((1 - \gamma) \mathbf{a}_i + \gamma \mathbf{a}_{i+1} \right) \tag{5}$$

define the Newmark approximations (Newmark (1959)) while

$$\mathbf{d}_0 = \mathbf{d}, \qquad \mathbf{v}_0 = \mathbf{v} \tag{6}$$

$$\mathbf{a}_0 = \mathbf{M}^{-1} \left(\mathbf{F}(0) - \mathbf{C}\mathbf{v}_0 - \mathbf{S}(\mathbf{d}_0) \right). \tag{7}$$

The time discrete combinations of displacements, velocities, accelerations and times read

$$\begin{aligned} \mathbf{d}_{i+1-\alpha_f} &= (1 - \alpha_f) \mathbf{d}_{i+1} + \alpha_f \mathbf{d}_i \\ \mathbf{v}_{i+1-\alpha_f} &= (1 - \alpha_f) \mathbf{v}_{i+1} + \alpha_f \mathbf{v}_i \\ \mathbf{a}_{i+1-\alpha_m} &= (1 - \alpha_m) \mathbf{a}_{i+1} + \alpha_m \mathbf{a}_i \end{aligned} \tag{8}$$

where $i \in \{0, 1, ..., m-1\}$, m is the number of time steps while $\mathbf{d}_i, \mathbf{v}_i$ and $\mathbf{a}_i$ are the numerical approximations of $\mathbf{u}(t_i)$, $\dot{\mathbf{u}}(t_i)$ and $\ddot{\mathbf{u}}(t_i)$, respectively. Usually, inertial and damping forces are linearly interpolated while $\mathbf{F}_{i+1-\alpha_f} = \mathbf{F}(\alpha_f, t_i, t_{i+1})$, is approximated by means of $\mathbf{F}_{i+1-\alpha_f} = (1-\alpha_f)\mathbf{F}(t_{i+1}) + \alpha_f \mathbf{F}(t_i)$ or $\mathbf{F}_{i+1-\alpha_f} = \mathbf{F}((1-\alpha_f)t_{i+1} + \alpha_f t_i)$. With regard to the non-linear internal forces $\mathbf{S}_{i+1-\alpha_f} = \mathbf{S}(\alpha_f, \mathbf{d}_i, \mathbf{d}_{i+1})$, three quadrature rules are considered in the foregoing:

the generalized trapezoidal rule (TR)

$$\mathbf{S}_{i+1-\alpha_f}^{TR} = (1-\alpha_f)\mathbf{S}(\mathbf{d}_{i+1}) + \alpha_f \mathbf{S}(\mathbf{d}_i); \tag{9}$$

the generalized mid-point rule (MR)

$$\mathbf{S}_{i+1-\alpha_f}^{MR} = \mathbf{S}[(1-\alpha_f)\mathbf{d}_{i+1} + \alpha_f \mathbf{d}_i]; \tag{10}$$

and the generalized energy-momentum rule $(GEMR)$

$$\mathbf{S}_{i+1-\alpha_f}^{GEMR} = \mathbf{S}(\alpha_f, \mathbf{d}_i, \mathbf{d}_{i+1}) \tag{11}$$

proposed by Kuhl and Crisfield (1999).

In principle, the algorithmic parameters α_m, α_f, β and γ of the $G-\alpha$ methods may be independent. Nonetheless, relations among them must be established to achieve consistency, stability and favourable dissipation properties. These relations are discussed for the $G-\alpha$ methods in the foregoing.

2.2 Linear three-step formulation

The Eqs. (3)-(5) allow $\mathbf{d}_{i+1}, \mathbf{v}_{i+1}$ and $\mathbf{a}_{i+1}$ to be determined starting from known values of $\mathbf{d}_i, \mathbf{v}_i$ and $\mathbf{a}_i$. If the same relations are applied to the time intervals $[t_{i+1}, t_{i+2}]$ and $[t_{i+2}, t_{i+3}]$, nine equations are obtained, in which four velocities and four accelerations can be eliminated. Thereby, a recurrence relation is obtained among displacements $\mathbf{d}_{i+j}$, $j = 0, 1, 2, 3$, that leads to the linear multistep (LMS) formulation of the $G-\alpha$ methods. As a result, the three-step algorithm is obtained

$$\sum_{j=0}^{3} \left[\mathbf{M}\alpha_j \mathbf{d}_{i+j} + \Delta t \mathbf{C}\gamma_j \mathbf{d}_{i+j}\right] + \Delta t^2 \sum_{j=1}^{3} \delta_j \left(\mathbf{S}_{i+j-\alpha_f} - \mathbf{F}_{i+j-\alpha_f}\right) = \mathbf{0} \tag{12}$$

where the parameters read

$$
\begin{array}{ccc}
\alpha_0 = \alpha_m & \gamma_0 = \alpha_f(-1+\gamma) & \delta_1 = \frac{1}{2} + \beta - \gamma \\
\alpha_1 = 1 - 3\alpha_m & \gamma_1 = -1 + 2\alpha_f + \gamma - 3\gamma\alpha_f & \delta_2 = \frac{1}{2} - 2\beta + \gamma \\
\alpha_2 = -2 + 3\alpha_m & \gamma_2 = 1 - \alpha_f - 2\gamma + 3\gamma\alpha_f & \delta_3 = \beta. \\
\alpha_3 = 1 - \alpha_m & \gamma_3 = (1 - \alpha_f)\gamma &
\end{array}
\tag{13}
$$

2.3 Effective structural equation

The Eqs. (3)-(5) can be combined in the following non-linear relation

$$
\begin{aligned}
& \mathbf{S}_{i+1-\alpha_f}\left(\mathbf{d}_{i+1}\right) - \mathbf{F}_{i+1-\alpha_f} \\
& -\mathbf{M}\left[-\frac{1-\alpha_m}{\beta\Delta t^2}\left(\mathbf{d}_{i+1} - \mathbf{d}_i\right) + \frac{1-\alpha_m}{\beta\Delta t}\mathbf{v}_i + \frac{1-\alpha_m-2\beta}{2\beta}\mathbf{a}_i\right] \\
& -\mathbf{C}\left[-\frac{(1-\alpha_f)\gamma}{\beta\Delta t}\left(\mathbf{d}_{i+1} - \mathbf{d}_i\right) + \frac{(1-\alpha_f)\gamma-\beta}{\beta}\mathbf{v}_i + \frac{(\gamma-2\beta)(1-\alpha_f)}{2\beta}\Delta t\mathbf{a}_i\right] = \mathbf{0}.
\end{aligned}
\tag{14}
$$

in the unknown displacement vector $\mathbf{d}_{i+1}$ which can be solved applying a consistent linearization and the Newton-Raphson method. Once $\mathbf{d}_{i+1}$ is computed, $\mathbf{a}_{i+1}$ and $\mathbf{v}_{i+1}$ can be determined using Eqs. (4) and (5), viz.

$$
\mathbf{a}_{i+1} = \frac{\mathbf{d}_{i+1} - \left(\mathbf{d}_i + \Delta t\mathbf{v}_i + \left(\frac{1}{2} - \beta\right)\Delta t^2\mathbf{a}_i\right)}{\beta\Delta t^2}
\tag{15}
$$

$$
\mathbf{v}_{i+1} = \mathbf{v}_i + (1-\gamma)\Delta t\mathbf{a}_i + \gamma\Delta t\mathbf{a}_{i+1}.
\tag{16}
$$

Details of these and other techniques used to solve non-linear dynamic problems involving material and geometric nonlinearities can be found in Karabalis and Beskos (1997).

3 Non-linear consistency

To analyse the consistency of the $G-\alpha$ methods in the non-linear regime, the approach exploited by Wood (1990, p. 20) is followed. The load vector $\mathbf{F}(t)$ is not included in the analysis assuming that the power of the leading error term of its approximation is greater than the order of accuracy of the methods. Starting from the LMS formulation (12), the difference operator $\mathbf{L}(\mathbf{d}, t, \Delta t)$ can be defined as

$$
\mathbf{L}(\mathbf{d}, t, \Delta t) = \frac{1}{\Delta t^2}\left[\sum_{j=0}^{3}\left[\mathbf{M}\alpha_j\mathbf{d}_{i+j} + \Delta t\mathbf{C}\gamma_j\mathbf{d}_{i+j}\right] + \Delta t^2\sum_{j=1}^{3}\delta_j\mathbf{S}_{i+j-\alpha_f}\right].
\tag{17}
$$

As the coefficients δ_j defined in (13) do not depend on the linearity of $\mathbf{S}(\mathbf{d})$, the extension of the consistency results from the linear to the non-linear regime is straightforward.

8

Hulbert and Hughes (1987) pointed out in the linear regime that the accelerations computed with the $HHT - \alpha$ method are only first order accurate, even though the relevant displacements are second order accurate. Hence, the consistency analysis both of displacements and accelerations evaluated with the $G - \alpha$ methods are considered in the foregoing.

3.1 Displacement

The local truncation error $\boldsymbol{\tau_u}(t, \Delta t)$ reads

$$\boldsymbol{\tau_u}(t, \Delta t) = \mathbf{L}(\mathbf{u}, t, \Delta t) = \mathbf{O}\left(\Delta t^k\right) \tag{18}$$

where $\mathbf{u} = \mathbf{u}(t)$ is a sufficiently smooth solution of the differential equation (1) and k, the order of the lowest term of the Taylor power series expansion of (18), the so-called order of accuracy. Expanding $\mathbf{u}(t_{i+j}) = \mathbf{u}(t_i + j\Delta t)$ by Taylor series about t_i in the Eq. (18) and collecting together terms with like powers of Δt, one obtains

$$\begin{aligned}
\boldsymbol{\tau_u}(t_i, \Delta t) =\ & \frac{1}{\Delta t^2}\mathbf{M}\mathbf{u}(t_i)\sum_{j=0}^{3}\alpha_j + \\
& +\frac{1}{\Delta t}\left[\mathbf{M}\frac{d\mathbf{u}(t_i)}{dt}\sum_{j=0}^{3}j\alpha_j + \mathbf{C}\mathbf{u}(t_i)\sum_{j=0}^{3}\gamma_j\right] + \\
& +\left[\mathbf{M}\frac{d^2\mathbf{u}(t_i)}{dt^2}\sum_{j=0}^{3}\frac{j^2}{2!}\alpha_j + \mathbf{C}\frac{d\mathbf{u}(t_i)}{dt}\sum_{j=0}^{3}j\gamma_j + \mathbf{S}[\mathbf{u}(t_i)]\sum_{j=1}^{3}\delta_j\right] + \\
& +\Delta t\left[\mathbf{M}\frac{d^3\mathbf{u}(t_i)}{dt^3}\sum_{j=0}^{3}\frac{j^3}{3!}\alpha_j + \mathbf{C}\frac{d^2\mathbf{u}(t_i)}{dt^2}\sum_{j=0}^{3}\frac{j^2}{2!}\gamma_j\right] + \\
& +\Delta t\frac{d\mathbf{S}[\mathbf{u}(t_i)]}{dt}\sum_{j=1}^{3}(j-\alpha_f)\delta_j + \\
& +\mathbf{O}(\Delta t^2).
\end{aligned} \tag{19}$$

Recalling (13), it is straightforward to prove that

$$\sum_{j=0}^{3}\alpha_j = \sum_{j=0}^{3}j\alpha_j = \sum_{j=0}^{3}\gamma_j = 0 \tag{20}$$

$$\sum_{j=0}^{3}\frac{j^2}{2!}\alpha_j = \sum_{j=0}^{3}j\gamma_j = \sum_{j=1}^{3}\delta_j = 1. \tag{21}$$

9

Therefore the $G - \alpha$ methods are consistent, viz. they exhibit accuracy at least equal to $\boldsymbol{\tau_u}(t_i, \Delta t) = \mathbf{O}(\Delta t)$. Further, the condition

$$\sum_{j=0}^{3} \frac{j^3}{3!}\alpha_j = \sum_{j=0}^{3} \frac{j^2}{2!}\gamma_j = \sum_{j=1}^{3} (j - \alpha_f)\beta_j \tag{22}$$

entails that the coefficient of Δt on the right-hand side of Eq. (19) vanishes. Thereby, from the Eqs. (13) and (22), the $G - \alpha$ methods have accuracy $\boldsymbol{\tau_u}(t_i, \Delta t) = \mathbf{O}\left(\Delta t^2\right)$, viz.

$$\mathbf{d}_i = \mathbf{u}(t_i) + \mathbf{O}\left(\Delta t^2\right) \tag{23}$$

provided that $\gamma = \frac{1}{2} - \alpha_m + \alpha_f$. Under this assumption, the $G - \alpha$ methods appear consistent with order two ($k = 2$) in the non-linear regime.

To warrant this analytical convergence rate estimate, two representative model problems described in detail in Section 6 are examined. They are a Duffing hardening oscillator endowed with a reaction force (80) shown in Fig. 1a and a non-linear clamped-free homogeneous elastic rod discretized with ten one-dimensional elements sketched in Fig. 2a. The relations among the parameters α_m, α_f, β and γ correspond to those exploited by the $CH - \alpha$ method (Chung and Hulbert (1993)). They are collected in row 5 of the Tables (2)-(3).

In the first problem, both the displacement error $|u(t_i) - d_i|$ and the velocity error $|\dot{u}(t_i) - v_i|$ were evaluated *a-posteriori* at a time level $t = 0.02$. Both errors and rates are depicted in Fig. 1b and 1c, respectively, where rules (9) and (10) have been used. The agreement between the analytical rate estimates and the test results is evident. Moreover, $\rho_\infty = 0$ entails $\alpha_f = 0$ according to Table (3), and therefore rules (9) and (10) coincide. Likewise, the same quantities are computed for node 10 of the non-linear rod. In this test, the *GEMR* rule (92) specialized to the non-linear rod is used. Again from Figs. 2b and 2c, both the displacement and the velocity error evaluated at a time level $t = 0.2$ exhibit a rate of two.

3.2 Acceleration

Hilber, Hughes and Taylor (1977) and Hulbert and Hughes (1987) pointed out that the numerical and the exact accelerations relevant to the $HHT - \alpha$ method satisfy the following relationship

$$\mathbf{a}_{i+1} - [(1 + \alpha_{HHT})\ddot{\mathbf{u}}(t_{i+1}) - \alpha_{HHT}\ddot{\mathbf{u}}(t_i)] = \mathbf{O}\left(\Delta t^2\right). \tag{24}$$

Eq. (24) implies that only a particular combination of the exact acceleration values is consistent and of order two. Hereinafter, the aforementioned result is extended to the $G-\alpha$ methods which satisfy the consistency condition $\gamma = \frac{1}{2} - \alpha_m + \alpha_f$, required to achieve second order accuracy with the displacements. Moreover, it is demonstrated that the acceleration evaluated with the $G-\alpha$ methods is consistent and of order one.

If $\mathbf{C} = \mathbf{0}$, the exact equilibrium equation (1) at time t_i reads

$$\mathbf{M\ddot{u}}\left(t_i\right) + \mathbf{S}\left(\mathbf{u}\left(t_i\right)\right) = \mathbf{0} \tag{25}$$

while the balance equation (3) becomes

$$\left(1 - \alpha_m\right)\mathbf{Ma}_{i+1} + \alpha_m\mathbf{Ma}_i + \mathbf{S}_{i+1-\alpha_f} = \mathbf{0}. \tag{26}$$

Substituting Eq. (23) in Eq. (26) one obtains

$$\left(1 - \alpha_m\right)\mathbf{Ma}_{i+1} + \alpha_m\mathbf{Ma}_i + \mathbf{S}_{i+1-\alpha_f}^{ex} = \mathbf{O}\left(\Delta t^2\right) \tag{27}$$

where $\mathbf{S}_{i+1-\alpha_f}^{ex} = \mathbf{S}\left(\alpha_f, \mathbf{u}\left(t_i\right), \mathbf{u}\left(t_{i+1}\right)\right)$. Eq. (27) holds for any approximation $\mathbf{S}_{i+1-\alpha_f} = \mathbf{S}_{i+1-\alpha_f}\left(\alpha_f, \mathbf{d}_i, \mathbf{d}_{i+1}\right)$ of the non-linear term which is assumed to be smooth with respect to $\mathbf{d}_i$ and $\mathbf{d}_{i+1}$. Substituting the relation $\mathbf{S}_{i+1-\alpha_f}^{ex} = \mathbf{S}_{i+1-\alpha_f}^{ex,TR} + \mathbf{O}\left(\Delta t^2\right)$ and Eq. (25) in the Eq. (27), the following relationship

$$\left[\left(1 - \alpha_m\right)\mathbf{a}_{i+1} + \alpha_m\mathbf{a}_i\right] - \left[\left(1 - \alpha_f\right)\mathbf{\ddot{u}}\left(t_{i+1}\right) + \alpha_f\mathbf{\ddot{u}}\left(t_i\right)\right] = \mathbf{O}\left(\Delta t^2\right) \tag{28}$$

is obtained. Eq. (28) represents the generalization of Eq. (24).

Setting $i = 0$ in Eq. (28) and recalling from Eqs. (6) and (7) that $\mathbf{a}_0 = \mathbf{\ddot{u}}\left(0\right)$ one obtains

$$\mathbf{\ddot{u}}\left(t_1\right) - \mathbf{a}_1 = \frac{\alpha_f - \alpha_m}{1 - \alpha_m}\left(\mathbf{\ddot{u}}\left(t_1\right) - \mathbf{\ddot{u}}\left(t_0\right)\right) + \mathbf{O}\left(\Delta t^2\right) \tag{29}$$

which can be expressed as follows

$$\mathbf{E}_1^{(a)} = \mathbf{c}_0^{(a)}\Delta t + \mathbf{O}\left(\Delta t^2\right)$$

if the exact solution $\mathbf{u}\left(t\right)$ is sufficiently smooth, with $\mathbf{E}_1^{(a)} = \mathbf{\ddot{u}}\left(t_1\right) - \mathbf{a}_1$ and $\mathbf{c}_0^{(a)} = \frac{\alpha_f - \alpha_m}{1 - \alpha_m}\mathbf{\dddot{u}}\left(t_0\right)$. At the $i-th$ step, Eq. (29) reads

$$\mathbf{\ddot{u}}\left(t_{i+1}\right) - \mathbf{a}_{i+1} = \frac{\alpha_f - \alpha_m}{1 - \alpha_m}\left(\mathbf{\ddot{u}}\left(t_{i+1}\right) - \mathbf{\ddot{u}}\left(t_i\right)\right) + \frac{-\alpha_m}{1 - \alpha_m}\left(\mathbf{\ddot{u}}\left(t_i\right) - \mathbf{a}_i\right) + \mathbf{O}\left(\Delta t^2\right)$$

and can be expressed as

$$\mathbf{E}_{i+1}^{(a)} = \mathbf{c}_i^{(a)} \Delta t + \eta \mathbf{E}_i^{(a)} + \mathbf{O}\left(\Delta t^2\right) \tag{30}$$

with $\mathbf{E}_i^{(a)} = \ddot{\mathbf{u}}(t_i) - \mathbf{a}_i$, $\mathbf{c}_i^{(a)} = \frac{\alpha_f - \alpha_m}{1 - \alpha_m} \dddot{\mathbf{u}}(t_i)$ and $\eta = \frac{-\alpha_m}{1 - \alpha_m}$.

Eq. (30) yields the following relation

$$\left\| \mathbf{E}_i^{(a)} \right\| \leqslant N \Delta t \sum_{j=0}^{i-1} \eta^j + \eta^i \|\mathbf{E}_0\| \tag{31}$$

in which $N = \max_{t_i \in [0, t_f]} \left\| \mathbf{c}_i^{(a)} \right\|$. Assuming that $\mathbf{E}_0 = \ddot{\mathbf{u}}(t_0) - \mathbf{a}_0 = \mathbf{0}$ and $\eta \neq 1$ the application of the discrete Gronwall lemma (Stuart and Humphries (1996), p. 9) to Eq. (31) implies

$$\left\| \mathbf{E}_i^{(a)} \right\| = \|\ddot{\mathbf{u}}(t_i) - \mathbf{a}_i\| \leqslant N \Delta t \frac{1 - \eta^{i+1}}{1 - \eta}. \tag{32}$$

If $|\eta| < 1 \iff \alpha_m < \frac{1}{2}$, the relation (32) entails

$$\ddot{\mathbf{u}}(t_i) - \mathbf{a}_i = \mathbf{O}\left(\Delta t\right), \tag{33}$$

viz. the computed acceleration is only first order accurate. If $\alpha_m = \frac{1}{2} \iff \eta = -1$ then Eq. (33) still holds. Conversely when $\alpha_m = \alpha_f$, as in row 2 of Table 2, then $N = 0$ and $\ddot{\mathbf{u}}(t_i) - \mathbf{a}_i = \mathbf{O}\left(\Delta t^2\right)$. As a result, the computed acceleration is second order accurate. Figs. 1d and 2d depict the convergence rate of the acceleration of the hardening system and of the non-linear elastic rod, respectively. Such rates confirm the analytical rate estimates inferred by Eq. (33).

4 Non-linear stability

The stability analysis of the $CH - \alpha$ method was carried out by Chung and Hulbert (1993) in the linear regime. More specifically, the concept of spectral stability was applied to the algorithm expressed as single-step three-stage method. As an alternative, the stability analysis could be performed exploiting the three-step form of the algorithm (Lambert (1991), p. 45). Nonetheless, no stability analysis of the $G - \alpha$ schemes has been conducted in the non-linear regime to the authors' knowledge. Moreover, as a M.D.o.F. non-linear system cannot be decomposed into n_{DoF} uncoupled scalar equations, stability analyses have to be necessarily performed on M.D.o.F. systems.

To tackle the stability analysis of the $G - \alpha$ methods, the following definitions of stability are considered hereinafter: (i) the G-stability notion applied in the context of p-step methods (Hairer and Wanner (1991), p. 332); (ii) the non-linear (energy) stability analysis suggested, among others, by Belytschko and Schoeberle (1975) and Hughes (1975), (1976) . Also the local stability analysis proposed by Park (1975) could be applied to these schemes. Nonetheless for brevity, such analysis is not illustrated as being restricted to S.D.o.F. systems.

For completeness, an additional stability analysis can be performed on Eq. (1): the so-called zero-stability analysis (Lambert (1991), p. 45) . This analysis is discussed briefly here, because it regards the stability of the difference system in the limit $\Delta t \to 0$. In this condition, the roots of (97) defined in Appendix 1 reduce to those of the polynomial $\rho(r) = \sum_{j=0}^{p} \alpha_j r^j$. The stability of the scheme requires that the roots exhibit modulus less or equal to unity while the roots with modulus equal to unity must possess multiplicity less than or equal to two ((Hairer, Nørsett and Wanner (1987), p. 424) . It can be proved readily by means of Eq. (13), that the aforementioned condition is satisfied if $\alpha_m \leqslant \frac{1}{2}$. Moreover, it is evident that the zero-stability notion is independent of the non-linearity of $\mathbf{S}(\mathbf{d})$ and $\mathbf{F}(t)$, Eq. (12) being only dependent on the parameters α_j for $\Delta t \to 0$.

4.1   Contractivity and G-stability

For *stiff* problems, the above-mentioned zero-stability notion represents only one necessary condition. As a matter of fact, a stability definition applicable to a fixed time step is needed. In recent years, the non-linear G-stability theory has emerged for non-linear contractive systems which requires that the numerical solutions of a linear multistep method be contractive in the G-norm (Hairer and Wanner (1991), p. 332).

Given a first order differential equation $\dot{\mathbf{y}} = \mathbf{f}(t, \mathbf{y})$ with any two solutions $\mathbf{y}$ and $\mathbf{z}$ satisfyng the initial conditions $\mathbf{y}(0) = \mathbf{y}_0$ and $\mathbf{z}(0) = \mathbf{z}_0$, respectively, the solutions are said to be contractive if and only if the system is dissipative, viz.

$$\langle \mathbf{f}(t, \mathbf{y}) - \mathbf{f}(t, \mathbf{y}), \mathbf{y} - \mathbf{z} \rangle \leq 0 \tag{34}$$

(Lambert (1991), p. 266), where $\langle \cdot, \cdot \rangle$ defines the inner product for which the corresponding norm is the standard L_2 norm. In the non-linear unforced case $\mathbf{F}(t) = \mathbf{0}$, it can be proved that

Eq. (1) does not satisfy Eq. (34). The usual first order form of Eq. (1) reads

$$\mathbf{y} = \begin{bmatrix} \mathbf{u}_y \\ \dot{\mathbf{u}}_y \end{bmatrix} \tag{35}$$

$$\dot{\mathbf{y}} = \mathbf{f}(t, \mathbf{y})) = \begin{bmatrix} \dot{\mathbf{u}}_y \\ \mathbf{M}^{-1}(-\mathbf{C}\dot{\mathbf{u}}_y - \mathbf{S}(\mathbf{u}_y)) \end{bmatrix}$$

where $\mathbf{u}_y$ and $\dot{\mathbf{u}}_y$ are the displacement and the velocity vectors, respectively, corresponding to the initial conditions $\mathbf{u}_{y0}$ and $\mathbf{v}_{y0}$. Conversely, if the $\mathbf{y}$ vector is defined as follows,

$$\mathbf{y} = \begin{bmatrix} \bar{\mathbf{K}}^{\frac{1}{2}} \mathbf{u}_y \\ \mathbf{M}^{\frac{1}{2}} \dot{\mathbf{u}}_y \end{bmatrix} \tag{36}$$

where $\bar{\mathbf{K}}$ is an arbitrary symmetric stiffness matrix, then Eq. (1) reads

$$\dot{\mathbf{y}} = \mathbf{f}(t, \mathbf{y})) = \begin{bmatrix} \bar{\mathbf{K}}^{\frac{1}{2}} \dot{\mathbf{u}}_y \\ \mathbf{M}^{\frac{1}{2}} \ddot{\mathbf{u}}_y \end{bmatrix} = \begin{bmatrix} \bar{\mathbf{K}}^{\frac{1}{2}} \dot{\mathbf{u}}_y \\ \mathbf{M}^{-1/2}(-\mathbf{C}\dot{\mathbf{u}}_y - \mathbf{S}(\mathbf{u}_y)) \end{bmatrix}.$$

If $\mathbf{z} = \left[\left(\bar{\mathbf{K}}^{\frac{1}{2}} \mathbf{u}_z \right)^T, \left(\mathbf{M}^{\frac{1}{2}} \dot{\mathbf{u}}_z \right)^T \right]^T$ with the initial conditions $\mathbf{u}_{z0}$ and $\mathbf{v}_{z0}$, it is straightforward to prove that

$$\langle \mathbf{f}(t, \mathbf{y}) - \mathbf{f}(t, \mathbf{z}), \mathbf{y} - \mathbf{z} \rangle = \left\langle \frac{d}{dt}(\mathbf{y} - \mathbf{z}), \mathbf{y} - \mathbf{z} \right\rangle = \frac{1}{2}\frac{d}{dt}\|\mathbf{y} - \mathbf{z}\|^2 \tag{37}$$

$$= \frac{1}{2}\frac{d}{dt}\left[(\mathbf{u}_y - \mathbf{u}_z)^T \bar{\mathbf{K}}(\mathbf{u}_y - \mathbf{u}_z) + (\dot{\mathbf{u}}_y - \dot{\mathbf{u}}_z)^T \mathbf{M}(\dot{\mathbf{u}}_y - \dot{\mathbf{u}}_z) \right]$$

$$= (\dot{\mathbf{u}}_y - \dot{\mathbf{u}}_z)^T \left[\bar{\mathbf{K}}(\mathbf{u}_y - \mathbf{u}_z) + \mathbf{M}(\ddot{\mathbf{u}}_y - \ddot{\mathbf{u}}_z) \right]$$

$$= (\dot{\mathbf{u}}_y - \dot{\mathbf{u}}_z)^T \left[-\mathbf{C}(\dot{\mathbf{u}}_y - \dot{\mathbf{u}}_z) - \Delta\mathbf{S}(\mathbf{u}_y, \mathbf{u}_z) \right]$$

where $\Delta\mathbf{S}(\mathbf{u}_y, \mathbf{u}_z) = \mathbf{S}(\mathbf{u}_y) - \mathbf{S}(\mathbf{u}_z) - \bar{\mathbf{K}}(\mathbf{u}_y - \mathbf{u}_z)$. In the linear case, $\mathbf{S}(\mathbf{u}) = \mathbf{K}\mathbf{u}$, and choosing $\bar{\mathbf{K}} = \mathbf{K}$ it is easy to demonstrate that $\Delta\mathbf{S}(\mathbf{u}_y, \mathbf{u}_z) = \mathbf{0}$. As a result, recalling that $\mathbf{C}$ is symmetric and positive semidefinite, the inequality (34) is satisfied. In the non-linear case, the sign of the term $\Delta\mathbf{S}(\mathbf{u}_y, \mathbf{u}_z)$ is in general undefined. Thereby, the relation (34) cannot be proved and the dynamical system may not be dissipative.

Fig. 3a shows the evolution provided by Eq. (34) for a Duffing hardening oscillator with $\bar{K} = S_1$, integrated with the $CH - \alpha$ method ($\rho_\infty = 1$), using the TR rule (9) and a very small time step size $\Delta t = 0.001$. It is evident that the relation (34) is satisfied only for the linear system endowed with $S_2 = 0$. Thereby, as the dynamical system (1) is generally non dissipative, only the non-linear (energy) stability analysis is conducted further.

4.2 Non-linear (energy) stability

A sufficient condition for the (energy) stability in the non-linear regime of an unforced system is provided by the following inequality

$$E_{i+1} \leqslant E_i \quad \Longleftrightarrow \quad \Delta E_i = E_{i+1} - E_i \leqslant 0 \tag{38}$$

which expresses the conservation or decay of the total energy within a time step (Kuhl and Crisfield (1999)). More specifically, $E_i = T_i + U_i = \frac{1}{2}\mathbf{v}_i^T \mathbf{M} \mathbf{v}_i + U(\mathbf{d}_i)$ defines the total mechanical energy of the system at the beginning of the *i-th* time step. The condition expressed by (38) is satisfied by the CAA method in the linear regime. Moreover, if the following inequality

$$\hat{E}_{i+1} \leqslant \hat{E}_i \quad \Longleftrightarrow \quad \Delta \hat{E}_i = \hat{E}_{i+1} - \hat{E}_i \leqslant 0 \tag{39}$$

is exploited, also the $N-\beta$ method satisfies the above-mentioned stability in energy in the linear regime. In detail, $\hat{E}_i = E_i + \Delta t^2 \left(\beta - \frac{\gamma}{2}\right) \frac{1}{2}\mathbf{a}_i^T \mathbf{M} \mathbf{a}_i$ is an energy norm which can be interpreted as a generalized energy (Wood (1990), p. 234).

In order to apply the same approach to the class of the $G - \alpha$ methods, the mean value operator $\langle \cdot \rangle$ and the undivided forward difference operator Δ are introduced, respectively. More specifically, $\langle g_i \rangle = \frac{g_i + g_{i+1}}{2}$ and $\Delta g_i = g_{i+1} - g_i$ where g_i is a scalar or a vector quantity. The procedure proposed by Hughes (1976) for the CAA scheme is applied to the $G - \alpha$ methods in the absence of damping and considering the classical TR rule (9). If $\mathbf{J_S}(\mathbf{d})$ is defined as the Jacobian operator of $\mathbf{S}(\mathbf{d})$, one gets

$$
\begin{aligned}
\Delta \hat{E}_i &= \Delta T_i + \Delta U_i + \Delta t^2 \left(\beta - \frac{\gamma}{2}\right) \Delta A_i \\
&= (\gamma - 1 + \alpha_m) \Delta \mathbf{d}_i^T \mathbf{M} \Delta \mathbf{a}_i \\
&\quad - \left(\frac{1}{2} - \alpha_f\right) \Delta \mathbf{d}_i^T \Delta \mathbf{S}_i \\
&\quad - \Delta t^2 \left(\gamma - \frac{1}{2}\right)\left(\beta - \frac{\gamma}{2}\right) \Delta \mathbf{a}_i^T \mathbf{M} \Delta \mathbf{a}_i + \Delta \mathbf{d}_i^T \mathbf{P}_i \Delta \mathbf{d}_i
\end{aligned}
\tag{40}
$$

where $\Delta T_i = \Delta \mathbf{v}_i \mathbf{M} \langle \mathbf{v}_i \rangle$, $\Delta A_i = \Delta \mathbf{a}_i \mathbf{M} \langle \mathbf{a}_i \rangle$, $\mathbf{S}_i = \mathbf{S}(\mathbf{d}_i)$, $\Delta U_i = \Delta U_{i,Lin} + \Delta U_{i,NLin} = \Delta \mathbf{d}_i^T \langle \mathbf{S}_i \rangle + \Delta \mathbf{d}_i^T \mathbf{P}_i \Delta \mathbf{d}_i$ and $\mathbf{P}_i = \frac{1}{4}\left(\mathbf{J_S}(\mathbf{d}_i^1) - \mathbf{J_S}(\mathbf{d}_i^2)\right)$. It is worthwhile to remark that the

error associated with the approximate solution of the non-linear Eq. (14) is assumed to be negligible in Eq. (40). As the terms in the rhs of Eq. (40) can be positive or negative according to the step i, the class of the $G - \alpha$ methods does not comply with the inequalities (38) and (39). Even the CAA scheme, characterized by $\alpha_m = \alpha_f = 0$ and $\gamma = 2\beta = \frac{1}{2}$ does not satisfy such inequalities as the relation (40) reads $\Delta \hat{E}_i = \Delta \mathbf{d}_i^T \mathbf{P}_i \Delta \mathbf{d}_i$. As a matter of fact, Hughes (1976) proved that $\Delta \hat{E}_i = \Delta E_i = \Delta \mathbf{d}_i^T \mathbf{P}_i \Delta \mathbf{d}_i$ and this term can be positive or negative. Moreover, Wood and Oduor (1988) proved that the term $\Delta \mathbf{d}_i^T \mathbf{P}_i \Delta \mathbf{d}_i$ of Eq. (40) can entail instability for a non-linear Duffing oscillator. Such phenomenon is highlighted in Fig. 3b, where the $CH - \alpha$ method with the TR rule (9) and $\rho_\infty = 1$ is applied to a softening Duffing oscillator characterized by the reaction force (84) and described in Section 6. Nonetheless, the particular choice $\rho_\infty = 0$, which corresponds to the asymptotic annihilation of the high-frequency response, is able to limit the instability phenomenon.

In the linear regime, Eq. (40) reads

$$
\begin{aligned}
\Delta \hat{E}_{i,Lin} &= (\gamma - 1 + \alpha_m) \, \Delta \mathbf{d}_i^T \mathbf{M} \Delta \mathbf{a}_i \\
&\quad - \left(\frac{1}{2} - \alpha_f \right) \Delta \mathbf{d}_i^T \mathbf{K} \Delta \mathbf{d}_i \\
&\quad - \Delta t^2 \left(\gamma - \frac{1}{2} \right) \left(\beta - \frac{\gamma}{2} \right) \Delta \mathbf{a}_i^T \mathbf{M} \Delta \mathbf{a}_i
\end{aligned}
\tag{41}
$$

and, again, the first term of the rhs can be positive or negative. Thereby, the inequality (39) is not satisfied. The growth and decay of the energy norm ratio $\hat{E}_{i,Lin} / \hat{E}_0$ provided by a linear undamped system with a natural frequency $\omega = 10$ using the $CH - \alpha$ method and the TR rule (9) is shown in Fig. 3c, where $\hat{E}_0$ represents the initial generalized energy. The numerical results confirm the analytical estimate of (41). In the particular case $\alpha_m = \alpha_f$, $\mathbf{M} \Delta \mathbf{a}_i = -\mathbf{K} \Delta \mathbf{d}_i$ and thereby,

$$
\begin{aligned}
\Delta \hat{E}_{i,Lin} &= - \left(\gamma - \frac{1}{2} \right) \Delta \mathbf{d}_i^T \mathbf{K} \Delta \mathbf{d}_i \\
&\quad - \Delta t^2 \left(\gamma - \frac{1}{2} \right) \left(\beta - \frac{\gamma}{2} \right) \Delta \mathbf{a}_i^T \mathbf{M} \Delta \mathbf{a}_i.
\end{aligned}
\tag{42}
$$

As a result, Eq. (42) satisfies (39). From the above-mentioned relationships, one concludes that the energy criterion expressed by the inequalities (38) or (39) is not applicable to the class of the $G - \alpha$ methods. Though these methods exhibit growth and decay of the mechanical

16

energy in the linear regime, it is possible to define a norm $\|\cdot\|_N$ of $\mathbf{X}_i = [\mathbf{d}_i, \mathbf{v}_i, \mathbf{a}_i]^T$ such that $\|\mathbf{X}_{i+1}\|_N \leqslant \|\mathbf{X}_i\|_N$ (Hughes 1987, p. 564). Thereby, the numerical norm decay of the discrete solution is enough for the $G - \alpha$ schemes to exhibit numerical stability.

5 Overshoot, high-frequency behaviour and numerical damping properties

The time step Δt of standard implicit algorithms employed in *stiff* differential equations is small compared to the period of the lower modes and large with respect to the period of high-frequency components. Numerical simulations of non-linear test problems display an asymptotic energy stability in the sense of Eq. (39) when $\Delta\tau = \frac{\Delta t}{T} \gg 1$, where T represents the period of the highest frequency component. See for instance Fig. 3d, which shows the generalized energy ratios $\frac{\hat{E}_{i+1}}{\hat{E}_i}$ as a function of $\Delta\tau = \frac{\Delta t}{T}$, provided by a Duffing hardening oscillator integrated with the $CH - \alpha$ method ($\rho_\infty = 0.5$) using the TR rule (9). On the other hand, Eq. (39) is violated for smaller values of $\Delta\tau$, which leads to the conclusion that the non-linear instability phenomena exhibited by the $G - \alpha$ methods are caused by the amplification of intermediate-frequency components. Along these lines, Hughes (1976) analysed the behaviour of the CAA method applied to the non-linear equation (1). More specifically, it was proved that the energy E is asymptotically conserved for $\Delta\tau \gg 1$. Another typical characteristic of the $G - \alpha$ methods in the condition $\Delta\tau \gg 1$ regards the numerical amplification of spurious high-frequency response components in the first steps also known as overshoot. Overshoot is clearly an undesirable feature of any numerical scheme applied to Eq. 1. It is widely discussed in literature, see e.g. Hilber and Hughes (1978) , Wood (1990) p. 134, among others, and it is independent of the algorithm stability. As far as the linear undamped case is concerned, Hilber and Hughes (1978) studied the overshoot effect of the $HHT - \alpha$ method by means of the asymptotic analysis. More recently, other methods based on the Rosenbrock algorithm and without overshoot have been compared to the $HHT - \alpha$ method (Piche (1995)). Nonetheless, no analysis of the aforementioned phenomena has been performed in the non-linear case to the best of the authors' knowledge. Such analyses are conducted hereinafter.

In order to analyse the overshoot phenomenon, Eq. (14) is considered in the unforced case

$\mathbf{F}(t) = \mathbf{0}$, for $i = 0$

$$\mathbf{S}_{1-\alpha_f}(\mathbf{d}_1) = \mathbf{M}\left[-\frac{1-\alpha_m}{\beta T^2 \Delta \tau^2}(\mathbf{d}_1 - \mathbf{d}_0) + \frac{1-\alpha_m - 2\beta}{2\beta}\mathbf{a}_0 + \frac{1-\alpha_m}{\beta T \Delta \tau}\mathbf{v}_0\right] \tag{43}$$

$$+\mathbf{C}\left[-\frac{(1-\alpha_f)\gamma}{\beta T \Delta \tau}(\mathbf{d}_1 - \mathbf{d}_0) + \frac{(\gamma - 2\beta)(1-\alpha_f)}{2\beta}T\Delta\tau\mathbf{a}_0 + \frac{(1-\alpha_f)\gamma - \beta}{\beta}\mathbf{v}_0\right],$$

along with Eqs. (4), (5) for $i = 0$

$$\mathbf{a}_1 = \left(1 - \frac{1}{2\beta}\right)\mathbf{a}_0 - \frac{1}{\beta T \Delta \tau}\mathbf{v}_0 + \frac{1}{\beta T^2 \Delta \tau^2}(\mathbf{d}_1 - \mathbf{d}_0) \tag{44}$$

$$\mathbf{v}_1 = \left(1 - \frac{\gamma}{2\beta}\right)\mathbf{a}_0 T\Delta\tau + \left(1 - \frac{\gamma}{\beta}\right)\mathbf{v}_0 + \frac{\gamma}{\beta T \Delta \tau}(\mathbf{d}_1 - \mathbf{d}_0). \tag{45}$$

Direct inspection of the Eq. (43) shows that the reaction force $\mathbf{S}_{1-\alpha_f}(\mathbf{d}_1)$ is of the same order of magnitude of $\Delta\tau$ when $\mathbf{C} \neq \mathbf{0}$, $\gamma \neq 2\beta$ and $\mathbf{a}_0 \neq \mathbf{0}$, being $\alpha_f \leq \frac{1}{2}$ (see row 2 of Table 1). This leads often to convergence problems of the Newton-Raphson algorithm employed for the computation of $\mathbf{d}_1$. Nonetheless, overshoot is clearly exhibited by $\mathbf{d}_1$ even in the case of convergent Newton-Raphson iterations. Thereby, $\mathbf{d}_1$ always assumes limited values and no overshoot in the displacements occurs when either $\mathbf{C} = \mathbf{0}$ or $\gamma = 2\beta$ or $\mathbf{a}_0 = \mathbf{0}$. Moreover, Eq. (45) shows clearly that $\mathbf{v}_1$ exhibits overshoot when $\gamma \neq 2\beta$ and $\mathbf{a}_0 \neq \mathbf{0}$ $\forall$ $\mathbf{C}$. It is also worthwhile to remark that the occurrence of overshoot only depends on the parameters β and γ included in (4) and (5), while it does not depend on the parameters α_m and α_f of Eq. (3). Hereinafter, an asymptotic analysis of the $G - \alpha$ methods for $\Delta\tau \gg 1$ is developed, which allows the high-frequency response properties of these algorithms to be studied in a unified framework, independently of the quadrature rules. Asymptotic expressions for $\{\mathbf{a}_i\}$, $\{\mathbf{v}_i\}$, $\{\mathbf{S}_{i+1-\alpha_f}\}$, $\{E_i\}$ and $\{\hat{E}_i\}$, are derived in the high-frequency limit, assuming that no overshoot in the displacements occurs.

When $\Delta\tau \gg 1$, the Eq. (43) can be simplified by omitting higher order terms in $\frac{1}{\Delta\tau}$. Moreover, for the sake of clarity, the parameters β and γ are expressed as functions of $\rho_\infty (\in [0, 1]$, where $\rho_\infty = 0$ asymptotic annihilation, $\rho_\infty = 1$ none), viz. $\beta = \frac{1}{(1+\rho_\infty)^2}$ and $\gamma = \frac{1}{2}\frac{3-\rho_\infty}{1+\rho_\infty}$, according to the relations of Table 3. Thus, one obtains

$$\mathbf{S}_{1-\alpha_f}(\mathbf{d}_1) = \mathbf{M}\left[\left(\frac{(1-\alpha_m)(1+\rho_\infty)^2}{2} - 1\right)\mathbf{a}_0 + \frac{(1-\alpha_m)(1+\rho_\infty)^2}{T\Delta\tau}\mathbf{v}_0\right] \tag{46}$$

$$+\mathbf{C}\left[-\frac{(1-\rho_\infty)^2(1-\alpha_f)}{4}T\Delta\tau\mathbf{a}_0 + \left(\frac{(1-\alpha_f)(3-\rho_\infty)(1+\rho_\infty)}{2} - 1\right)\mathbf{v}_0\right]$$

where the dependency of α_m and α_f on ρ_∞ is collected in Table 3.

The case $\rho_\infty \in [0,1)$ equivalent to $\gamma \neq 2\beta$ is analysed first. In this condition, overshoot in $\mathbf{d}$ can be avoided only in the following three cases:

$$
\begin{array}{lll}
\text{(a)} & \mathbf{a}_0 \neq \mathbf{0} & \mathbf{C} = \mathbf{0} \\
\text{(b)} & \mathbf{a}_0 = \mathbf{0} & \mathbf{C} = \mathbf{0} \\
\text{(c)} & \mathbf{a}_0 = \mathbf{0} & \mathbf{C} \neq \mathbf{0}
\end{array}
\tag{47}
$$

which imply the annihilation of the term $\mathbf{C}\frac{(1-\rho_\infty)^2(1-\alpha_f)}{4}T\Delta\tau\mathbf{a}_0$ in Eq. (46). As a result, this relation becomes

$$
\begin{aligned}
\mathbf{S}_{1-\alpha_f}(\mathbf{d}_1) \;=\;\; & \mathbf{M}\left[\left(\frac{(1-\alpha_m)(1+\rho_\infty)^2}{2} - 1\right)\mathbf{a}_0 + \frac{(1-\alpha_m)(1+\rho_\infty)^2}{T\Delta\tau}\mathbf{v}_0\right] \\
& +\mathbf{C}\left[\frac{(1-\alpha_f)(3-\rho_\infty)(1+\rho_\infty)}{2} - 1\right]\mathbf{v}_0,
\end{aligned}
$$

while Eqs. (44), (45) can be rewritten accordingly as

$$
\mathbf{a}_1 \;=\; \frac{1-2\rho_\infty-\rho_\infty^2}{2}\mathbf{a}_0 - \frac{(1+\rho_\infty)^2}{T\Delta\tau}\mathbf{v}_0
\tag{48}
$$

$$
\mathbf{v}_1 \;=\; \frac{(1-\rho_\infty)^2}{4}\mathbf{a}_0 T\Delta\tau - \frac{1+2\rho_\infty-\rho_\infty^2}{2}\mathbf{v}_0.
\tag{49}
$$

For the subsequent time step $(i=1)$ and considering that $\Delta\tau \gg 1$, Eq. (14) can be simplified by the same approximations performed for $i=0$, thus yielding

$$
\begin{aligned}
\mathbf{S}_{2-\alpha_f}(\mathbf{d}_2) \;=\;\; & \mathbf{M}\left[\left(\frac{(1-\alpha_m)(1+\rho_\infty)^2}{2} - 1\right)\mathbf{a}_1 + \frac{(1-\alpha_m)(1+\rho_\infty)^2}{T\Delta\tau}\mathbf{v}_1\right] \\
& +\mathbf{C}\left[-\frac{(1-\rho_\infty)^2(1-\alpha_f)}{4}T\Delta\tau\mathbf{a}_1 + \left(\frac{(1-\alpha_f)(3-\rho_\infty)(1+\rho_\infty)}{2} - 1\right)\mathbf{v}_1\right].
\end{aligned}
\tag{50}
$$

Accounting for the assumptions exploited in (47) and (48), it can be readily demonstrated that $\mathbf{d}_2$ is limited. Thereby, Eqs. (4) and (5) considered for $i=1$ and $\Delta\tau \gg 1$ yield

$$
\mathbf{a}_2 \;=\; \frac{1-2\rho_\infty-\rho_\infty^2}{2}\mathbf{a}_1 - \frac{(1+\rho_\infty)^2}{T\Delta\tau}\mathbf{v}_1
\tag{51}
$$

$$
\mathbf{v}_2 \;=\; \frac{(1-\rho_\infty)^2}{4}\mathbf{a}_1 T\Delta\tau - \frac{1+2\rho_\infty-\rho_\infty^2}{2}\mathbf{v}_1.
\tag{52}
$$

The following relations can then be determined iteratively

$$
\mathbf{a}_{i+1} \;=\; \frac{1-2\rho_\infty-\rho_\infty^2}{2}\mathbf{a}_i - \frac{(1+\rho_\infty)^2}{T\Delta\tau}\mathbf{v}_i
\tag{53}
$$

$$
\mathbf{v}_{i+1} \;=\; \frac{(1-\rho_\infty)^2}{4}\mathbf{a}_i T\Delta\tau - \frac{1+2\rho_\infty-\rho_\infty^2}{2}\mathbf{v}_i
\tag{54}
$$

19

for $i \geq 0$. Applying Eq. (53) and (54) to two subsequent time steps, the recursive relations

$$\mathbf{a}_{i+1} = -2\rho_\infty \mathbf{a}_i - \rho_\infty^2 \mathbf{a}_{i-1} \tag{55}$$

$$\mathbf{v}_{i+1} = -2\rho_\infty \mathbf{v}_i - \rho_\infty^2 \mathbf{v}_{i-1} \tag{56}$$

are obtained. As a result, by recursion on Eq. (55) and (56) and recalling the initial values expressed in (48) and (49), one obtains:

$$\{\mathbf{a}_i\} = (-1)^i \rho_\infty^{i-1} \left[\rho_\infty - \frac{i}{2} \left(1 - \rho_\infty^2\right) \right] \mathbf{a}_0 + i \, (-1)^i \, \rho_\infty^{i-1} \frac{(1 + \rho_\infty)^2}{T \Delta \tau} \mathbf{v}_0 \tag{57}$$

$$\{\mathbf{v}_i\} = -\frac{i}{4} (-1)^i \rho_\infty^{i-1} (1 - \rho_\infty)^2 \, \mathbf{a}_0 T \Delta \tau$$
$$- (-1)^i \rho_\infty^{i-1} \left[i \frac{\rho_\infty^2 - 2\rho_\infty - 1}{2} + (i-1)\rho_\infty \right] \mathbf{v}_0. \tag{58}$$

It is worthwhile to remark that the terms proportional to $\mathbf{a}_0$ in (58) will be dominant when $\Delta \tau \gg 1$. Therefore, the terms proportional to $\mathbf{v}_0$ will only be considered in the case $\mathbf{a}_0 = \mathbf{0}$. Substituting the values of $\mathbf{a}_i$ and $\mathbf{v}_i$ of Eq. (57) and (58), in Eq. (3) considered for $\mathbf{F}_{i+1-\alpha_f} = \mathbf{0}$, one obtains

$$\{\mathbf{S}_{i+1-\alpha_f}\} = (-1)^i \rho_\infty^{i-1} \left[\begin{array}{c} \left(-\rho_\infty + \frac{i}{2}\left(1 - \rho_\infty^2\right)\right)\left(-\rho_\infty\left(1 - \alpha_m\right) + \alpha_m\right) \\ -\frac{1}{2}\rho_\infty\left(1 - \rho_\infty^2\right)\left(1 - \alpha_m\right) \end{array} \right] \mathbf{M}\mathbf{a}_0$$
$$+ (-1)^i \rho_\infty^{i-1} \left[\rho_\infty \left(1 - \alpha_m\right)(i+1) - i \, \alpha_m \right] \frac{(1 + \rho_\infty)^2}{T \Delta \tau} \mathbf{M}\mathbf{v}_0$$
$$+ (-1)^i \rho_\infty^{i-1} \frac{(1 - \rho_\infty)^2}{4} \left[-\rho_\infty \left(1 - \alpha_f\right)(i+1) + \alpha_f \, i \right] \mathbf{C}\mathbf{a}_0 T \Delta \tau$$
$$+ (-1)^i \rho_\infty^{i-1} \left[\begin{array}{c} -\left(1 - \alpha_f\right)\rho_\infty \left[(i+1) \frac{\rho_\infty^2 - 2\rho_\infty - 1}{2} + i\rho_\infty \right] \\ + \alpha_f \left[i\frac{\rho_\infty^2 - 2\rho_\infty - 1}{2} + (i-1)\rho_\infty \right] \end{array} \right] \mathbf{C}\mathbf{v}_0. \tag{59}$$

Employing Eqs. (57) and (58) along the same lines, the asymptotic expressions for the sequences $\{E_i\}$ and $\left\{\hat{E}_i\right\}$ can be derived:

$$\{E_i\} = \rho_\infty^{2(i-1)} i^2 \frac{(1 - \rho_\infty)^4}{16} T^2 \Delta \tau^2 \frac{1}{2} \mathbf{a}_0^T \mathbf{M}\mathbf{a}_0$$
$$+ 2 \, i \, \rho_\infty^{2(i-1)} \frac{(1 - \rho_\infty)^2}{4} \left[i \frac{\rho_\infty^2 - 2\rho_\infty - 1}{2} + (i-1)\rho_\infty \right] T \Delta \tau \frac{1}{2} \mathbf{a}_0^T \mathbf{M}\mathbf{v}_0$$
$$+ \rho_\infty^{2(i-1)} \left[i \frac{\rho_\infty^2 - 2\rho_\infty - 1}{2} + (i-1)\rho_\infty \right]^2 \frac{1}{2} \mathbf{v}_0^T \mathbf{M}\mathbf{v}_0$$
$$+ U(\mathbf{d}_i) \tag{60}$$

20

and

$$
\begin{aligned}
\left\{\hat{E}_i\right\} &= \rho_\infty^{2(i-1)} \left[i^2 \frac{(1-\rho_\infty)^4}{16} + \frac{(1-\rho_\infty)^2}{4(1+\rho_\infty)^2} \left(-\rho_\infty + \frac{i}{2}\left(1-\rho_\infty^2\right)\right)^2\right] T^2 \Delta\tau^2 \frac{1}{2} \mathbf{a}_0^T \mathbf{M} \mathbf{a}_0 \\
&\quad + 2\, i\, \rho_\infty^{2(i-1)} \frac{(1-\rho_\infty)^2}{4} \left[i \frac{\rho_\infty^2 - 2\rho_\infty - 1}{2} + (i-1)\rho_\infty\right] T\Delta\tau \frac{1}{2} \mathbf{a}_0^T \mathbf{M} \mathbf{v}_0 \\
&\quad + \rho_\infty^{2(i-1)} \left[\left(i \frac{\rho_\infty^2 - 2\rho_\infty - 1}{2} + (i-1)\rho_\infty\right)^2 + \frac{i^2}{4}\left(1-\rho_\infty^2\right)^2\right] \frac{1}{2} \mathbf{v}_0^T \mathbf{M} \mathbf{v}_0 \\
&\quad + U\left(\mathbf{d}_i\right).
\end{aligned}
\tag{61}
$$

It is worthwhile to emphasize that $\{E_i\}$ and $\left\{\hat{E}_i\right\}$ can only be computed explicitly by means of the above-mentioned formulae as long as $U\left(\mathbf{d}_i\right)$ is negligible compared to the remaining term of the rhss for $i \geqslant 1$. It can be demonstrated that this holds as long as $\mathbf{C} = \mathbf{0}$ (cases (a) and (b) in (47)).

The asymptotic sequences of the ratios $r_{a,i}$, $r_{v,i}$, $r_{s,i}$, E_i/E_1 and $\hat{E}_i/\hat{E}_0$ relevant to case (a) in (47) are plotted in Fig. 4 and 5, for $\rho_\infty = 0.5$ and $\rho_\infty = 0.9$, respectively. More specifically, $\mathbf{a}_i = r_{a,i}\mathbf{a}_0$, $\mathbf{v}_i = r_{v,i}\mathbf{v}_1$ and $\mathbf{S}_{i+1-\alpha_f} = r_{s,i}\mathbf{S}_{1-\alpha_f}$ while the cases in which overshoot occurs according to the analysis performed above are pointed out. For this reason, the reference values for $\mathbf{v}_i$ and E_i are assumed to be $\mathbf{v}_1$ and E_1, respectively. It can be observed that all the ratios annihilate after a certain number i of time steps while this trend is faster for $\rho_\infty = 0.5$. Moreover, only $r_{s,i}$ depends upon the integration method employed as (59) exploits α_m and α_f which depend on ρ_∞ (see Table 3); all the sequences are independent on the quadrature rules (9)-(11).

The same ratios relevant to cases (b) and (c) in (47) are illustrated in Fig. 6 and 7, for $\rho_\infty = 0.5$ and $\rho_\infty = 0.9$, respectively. As $\mathbf{a}_0 = \mathbf{0}$, the plotted quantity $r_{a,i}$ is defined as $\mathbf{a}_i = r_{a,i}\mathbf{a}_1$ and the cases in which the ratios depend on $\Delta\tau^{-1}$ are pointed out too. All the ratios annihilate after a certain number i of time steps while the annihilation is faster for $\rho_\infty = 0.5$. Again, the ratios do not depend on the quadrature rule employed. In the next section, such analytical estimates are warranted by numerical simulations.

The sequences computed above allow the dissipation properties of the $G-\alpha$ methods relevant to the high-frequency components to be understood. In the linear regime, such properties are related to the spectral radius ρ_∞ as illustrated in Appendix 1. Hereinafter, it is shown that this

dependence on ρ_∞ also holds in the non-linear regime. From Eq. (57), in the limit $\Delta\tau \gg 1$, one gets

$$
\begin{aligned}
\frac{r_{a,i+1}}{r_{a,i}} &= \frac{\rho_\infty\left(-\rho_\infty + \frac{i+1}{2}\left(1-\rho_\infty^2\right)\right)}{\rho_\infty - \frac{i}{2}\left(1-\rho_\infty^2\right)} && \mathbf{a}_0 \neq \mathbf{0} \quad (i \geqslant 0) \\
\frac{r_{a,i+1}}{r_{a,i}} &= -\rho_\infty \frac{i+1}{i} && \mathbf{a}_0 = \mathbf{0} \quad (i \geqslant 1) \\
\lim_{i\to\infty} \frac{r_{a,i+1}}{r_{a,i}} &= -\rho_\infty && (62)
\end{aligned}
$$

Analogous results hold for the velocities through Eq. (58), and reaction forces through Eq. (59). As far as the energy ratios are concerned, on the basis of Eq. (60) and $\mathbf{C} = \mathbf{0}$ it is straightforward to prove that

$$
\frac{E_{i+1}}{E_i} = \rho_\infty^2 \frac{(i+1)^2}{i^2} \qquad \mathbf{a}_0 \neq \mathbf{0} \quad (i \geqslant 1) \tag{63}
$$

$$
\frac{E_{i+1}}{E_i} = \rho_\infty^2 \left[\frac{(i+1)\frac{\rho_\infty^2 - 2\rho_\infty - 1}{2} + i\,\rho_\infty}{i\frac{\rho_\infty^2 - 2\rho_\infty - 1}{2} + (i-1)\,\rho_\infty}\right]^2 \qquad \mathbf{a}_0 = \mathbf{0} \quad (i \geqslant 0). \tag{64}
$$

An attentive reader can observe that $\frac{E_{i+1}}{E_i}$ is not always bounded by 1. However, it can be proved that

$$
\lim_{i\to\infty} \frac{E_{i+1}}{E_i} = \rho_\infty^2. \tag{65}
$$

Analogously in the undamped case, Eq. (61) yields

$$
\frac{\hat{E}_{i+1}}{\hat{E}_i} = \rho_\infty^2 \frac{(i+1)^2 \frac{(1-\rho_\infty)^4}{16} + \frac{(1-\rho_\infty)^2}{4(1+\rho_\infty)^2}\left(-\rho_\infty + \frac{i+1}{2}\left(1-\rho_\infty^2\right)\right)^2}{i^2 \frac{(1-\rho_\infty)^4}{16} + \frac{(1-\rho_\infty)^2}{4(1+\rho_\infty)^2}\left(-\rho_\infty + \frac{i}{2}\left(1-\rho_\infty^2\right)\right)^2} \qquad \mathbf{a}_0 \neq \mathbf{0} \quad (i \geqslant 0) \tag{66}
$$

and

$$
\frac{\hat{E}_{i+1}}{\hat{E}_i} = \rho_\infty^2 \frac{\left((i+1)\frac{\rho_\infty^2 - 2\rho_\infty - 1}{2} + i\rho_\infty\right)^2 + \frac{(i+1)^2}{4}\left(1-\rho_\infty^2\right)^2}{\left(i\frac{\rho_\infty^2 - 2\rho_\infty - 1}{2} + (i-1)\,\rho_\infty\right)^2 + \frac{i^2}{4}\left(1-\rho_\infty^2\right)^2} \qquad \mathbf{a}_0 = \mathbf{0} \quad (i \geqslant 0). \tag{67}
$$

Thereby

$$
\frac{\hat{E}_{i+1}}{\hat{E}_i} \in [0,1) \tag{68}
$$

always holds for $\rho_\infty < 1$ and $\Delta\tau \gg 1$. Moreover,

$$
\lim_{i\to\infty} \frac{\hat{E}_{i+1}}{\hat{E}_i} = \rho_\infty^2. \tag{69}
$$

One can observe that Eqs. (63)-(69) do not depend on the algorithmic parameters α_m and α_f as well as on the internal force function $\mathbf{S} = \mathbf{S}(\mathbf{u})$. Eqs. (65) and (69) show clearly that the dissipation rate of high-frequency components is governed by ρ_∞ also in the non-linear regime. The ratios E_{i+1}/E_i and $\hat{E}_{i+1}/\hat{E}_i$, as functions of ρ_∞, are plotted in Fig. 8 both for the case $\mathbf{a}_0 \neq \mathbf{0}$ and $\mathbf{a}_0 = \mathbf{0}$, respectively. The convergence of those ratios to the limiting value ρ_∞^2 for $i \gg 1$ is evident.

The case $\rho_\infty = 1$ is considered hereinafter. It is worthwhile to recall that the non-dissipative CAA method, endowed with $\gamma = 2\beta = \frac{1}{2}$ and $\alpha_m = \alpha_f = 0$, was analysed by Hughes (1976) and Wood and Oduor (1988) . With regard to the $G - \alpha$ methods using $\rho_\infty = 1$, one obtains $\gamma = 2\beta = \frac{1}{2}$ according to Table 3 and

$$
\begin{array}{llllll}
1) & \alpha_m & = & \alpha_f = 0 & \text{for the} & N - \beta, HHT - \alpha, WBZ - \alpha \text{ methods} & (70)
\end{array}
$$

$$
\begin{array}{llllll}
2) & \alpha_m & = & \alpha_f = \dfrac{1}{2} & \text{for the} & CH - \alpha \text{ method.} & (71)
\end{array}
$$

In what follows, the asymptotic analysis is carried out as in the previous case ($\rho_\infty < 1$). When $\rho_\infty = 1$ Eq. (43) yields

$$
\mathbf{S}_{1-\alpha_f}(\mathbf{d}_1) = (1 - 2\alpha_m)\,\mathbf{M}\mathbf{a}_0 + (1 - \alpha_m)\frac{4}{T\Delta\tau}\mathbf{M}\mathbf{v}_0 + (1 - 2\alpha_f)\,\mathbf{C}\mathbf{v}_0
$$

and thereby,

$$
\begin{array}{lllll}
1) & \mathbf{S}_1(\mathbf{d}_1) & = & \mathbf{S}(\mathbf{d}_1) = \mathbf{M}\mathbf{a}_0 + \dfrac{4}{T\Delta\tau}\mathbf{M}\mathbf{v}_0 + \mathbf{C}\mathbf{v}_0 = -\mathbf{S}(\mathbf{d}_0) + \dfrac{4}{T\Delta\tau}\mathbf{M}\mathbf{v}_0 & (72)
\end{array}
$$

$$
\begin{array}{lllll}
2) & \mathbf{S}_{1-\frac{1}{2}}(\mathbf{d}_1) & = & \mathbf{S}_{1-\frac{1}{2}}(\mathbf{d}_0, \mathbf{d}_1) = \dfrac{2}{T\Delta\tau}\mathbf{M}\mathbf{v}_0 & (73)
\end{array}
$$

in the conditions (70) and (71), respectively. Two separated cases must be considered:

$$
\begin{array}{lll}
\text{(a)} & \mathbf{d}_0 = \mathbf{0} & \\
\text{(b)} & \mathbf{d}_0 \neq \mathbf{0}. &
\end{array} \tag{74}
$$

In the case (a) $\mathbf{v}_0 \neq \mathbf{0}$ must hold. It can be also proved through the Eqs. (72) and (73) that $\mathbf{d}_1$ is asymptotically negligible in this case, so that Eqs. (44) and (45) yield

$$
\begin{aligned}
\mathbf{a}_1 & = -\mathbf{a}_0 - \frac{4}{T\Delta\tau}\mathbf{v}_0 \\
\mathbf{v}_1 & = -\mathbf{v}_0.
\end{aligned}
$$

By iteration, one obtains

$$
\begin{aligned}
\{\mathbf{a}_i\} &= (-1)^i \mathbf{a}_0 + i (-1)^i \frac{4}{T\Delta\tau} \mathbf{v}_0 \\
\{\mathbf{v}_i\} &= (-1)^i \mathbf{v}_0 \\
\{E_i\} &= \left\{\hat{E}_i\right\} = \frac{1}{2}\mathbf{v}_0^T \mathbf{M}\mathbf{v}_0 = E_0 = \hat{E}_0
\end{aligned}
$$

$$
\text{1)} \qquad \{\mathbf{S}_{i+1}\} = (-1)^i (i+1) \frac{4}{T\Delta\tau} \mathbf{M}\mathbf{v}_0
$$

$$
\text{2)} \qquad \left\{\mathbf{S}_{i+1-\frac{1}{2}}\right\} = (-1)^i \frac{2}{T\Delta\tau} \mathbf{M}\mathbf{v}_0. \tag{75}
$$

In the case (b), Eqs. (72) and (73)

$$
\text{1)} \qquad \mathbf{S}(\mathbf{d}_1) = -\mathbf{S}(\mathbf{d}_0) + \frac{4}{T\Delta\tau} \mathbf{M}\mathbf{v}_0 \tag{76}
$$

$$
\text{2)} \qquad \mathbf{S}_{1-\frac{1}{2}}(\mathbf{d}_0, \mathbf{d}_1) = \frac{2}{T\Delta\tau} \mathbf{M}\mathbf{v}_0 \tag{77}
$$

are considered again. Nonetheless, the value of $\mathbf{d}_1$ can be easily determined from Eq. (76) under the assumption that $\mathbf{S}(-\mathbf{u}) = -\mathbf{S}(\mathbf{u})$ (see Hughes (1976)). As a result, one gets in the limit,

$$
\mathbf{d}_1 = -\mathbf{d}_0. \tag{78}
$$

On the other hand, if $\mathbf{S}_{1-\frac{1}{2}}(\mathbf{d}_0, \mathbf{d}_1) = \mathbf{S}_{1-\frac{1}{2}}^{TR}(\mathbf{d}_0, \mathbf{d}_1) = \frac{\mathbf{S}(\mathbf{d}_0)+\mathbf{S}(\mathbf{d}_1)}{2}$, through Eq. (77) it is easy to prove that $\mathbf{S}(\mathbf{d}_1) = -\mathbf{S}(\mathbf{d}_0) + \frac{4}{T\Delta\tau}\mathbf{M}\mathbf{v}_0$; thereby, the antisymmetry of $\mathbf{S}(\mathbf{u})$ implies again (78). The same result holds for all the quadrature rules for which $\mathbf{S}_{1-\frac{1}{2}}(\mathbf{d}_0, \mathbf{d}_1) = \mathbf{0}$ implies $\mathbf{S}(\mathbf{d}_1) = -\mathbf{S}(\mathbf{d}_0)$. Under these assumptions, Eqs. (44), (45) and (78) yield

$$
\begin{aligned}
\mathbf{a}_1 &= -\mathbf{a}_0 - \frac{4}{T\Delta\tau} \mathbf{v}_0 \\
\mathbf{v}_1 &= -\mathbf{v}_0 - \frac{4}{T\Delta\tau} \mathbf{d}_0.
\end{aligned}
$$

Thereby, by iteration for $i > 1$ it is easy to demonstrate that

$$
\begin{aligned}
\{\mathbf{d}_i\} &= (-1)^i \mathbf{d}_0 \\
\{\mathbf{a}_i\} &= (-1)^i \mathbf{a}_0 + i (-1)^i \frac{4}{T\Delta\tau} \mathbf{v}_0 \\
\{\mathbf{v}_i\} &= (-1)^i \mathbf{v}_0 + i (-1)^i \frac{4}{T\Delta\tau} \mathbf{d}_0 \\
\{E_i\} &= \left\{\hat{E}_i\right\} \to \frac{1}{2}\mathbf{v}_0^T \mathbf{M}\mathbf{v}_0 + U(\mathbf{d}_0) = E_0 = \hat{E}_0
\end{aligned} \tag{79}
$$

24

To warrant the analytical estimates provided by (79), the Duffing hardening oscillator endowed with the reaction force (80) and period T is considered. It has been integrated by means of the $CH - \alpha$ method with $\rho_\infty = 1$, using the TR rule (9) and a large time step size $\Delta t = 151.53$, viz. $\Delta t/T = 1000$. It is evident from Fig. 9, how energy E_i ($= \hat{E}_i$) is asymptotically conserved for small $i/(T\Delta\tau)$ ratios in agreement with the conclusions of Hughes (1976) and Hoff and Pahl (1988b).

6 Representative numerical simulations

In this section, three representative numerical examples are introduced both to evaluate the performance of the class of $G - \alpha$ methods and to warrant the analytical findings presented in the previous sections. The model problems selected exhibit key features typical of more complex systems which arise in non-linear structural dynamics.

The first problem deals with a S.D.o.F. system which is an unforced and undamped Duffing oscillator (Wood (1988) and (1990), p. 298). It can reproduce, for instance, the motion of a lumped mass attached to a taut string, viz. a hardening system.

The restoring force for such oscillator reads

$$S\left(u(t)\right) = S_1 u(t)(1 + S_2 u(t)^2) \tag{80}$$

where S_1 and S_2 are stiffness constants. Since a hardening system is examined, $S_2 > 0$. In order to analyse the time-stepping method it is useful to provide the solution of Eq. (1) with $M = 1$, $C = 0$ and $F(t) = 0$. As the non-linear term in the internal force is cubic in u, the solution can be easily expressed in terms of Jacobi elliptic functions (Wood (1988)). Let $K\left(m\right) = \int_0^{\frac{\pi}{2}} \frac{d\vartheta}{\sqrt{1 - m \sin^2 \vartheta}}$ denote the complete elliptic integral of the first kind (Abramowitz and Stegun (1964) p. 569) and consider the case of $\mathrm{v}_0 = 0$. The solution of the hardening system reads

$$u(t) = u_0 cn(-\hat{\omega}t, m) \tag{81}$$

$$\dot{u}(t) = u_0 \hat{\omega} sn(-\hat{\omega}t, m) dn(-\hat{\omega}t, m) \tag{82}$$

where $\hat{\omega}^2 = S_1(1 + S_2 u_0^2)$ and $m = S_2 u_0^2 / \left(2 + 2S_2 u_0^2\right)$. The solution is periodic with period

$$T = \frac{4K\left(m\right)}{\hat{\omega}}. \tag{83}$$

25

$S_1 = 100$, $S_2 = 10$, $u_0 = 1.5$ and $v_0 = 0$ was assumed in the simulations while according to the expression (83), the period of the solution appears to be $T = 0.15153$. Moreover, simulations on the softening oscillator analysed by Park (1975) and characterized by the reaction force

$$S\left(u(t)\right) = S_1 \tanh u(t) \tag{84}$$

with $S_1 = 100$ have also been performed.

The second problem regards a non-linear 2.D.o.F. system endowed with natural frequencies typical of large systems, introduced so as to highlight the favourable accuracy and dissipative properties of the higher modes of the proposed schemes. A linear version of this system was considered in Hughes ((1987), p. 542). The system is represented in Fig. 10 and is endowed with $m_1 = m_2 = 1$ and $\mathbf{C} = \mathbf{0}$. The restoring force $S_1\left(u_1\right)$ complies with Eq. (80), where $S_1 = S_2 = 10^4$ while $S_2\left(u_2\right)$ complies with Eq. (84) where $S_1 = 1$. The natural frequencies of the linear system are ω_1=0.99995 and ω_2=100.00500, respectively. The mode related to the lower frequency represents those modes that are physically important and must be accurately integrated. The second mode represents those spurious high-frequency modes which have to be filtered by the numerical method.

The results provided by the $CH - \alpha$ method using $\rho_\infty = 0.5$ and a time step size $\Delta t = 0.25$ are illustrated in Fig. 11. The initial conditions $\mathbf{u}_0^T = \{1.5,\ 2.5\}$ and $\mathbf{v}_0^T = \{0,\ 1\}$ entail $\mathbf{a}_0 \neq 0$ while the following expressions

$$E_{1,i} = \frac{1}{2}v_{1,i}^2 + \frac{1}{2}10^4 d_{1,i}^2 + \frac{1}{4}10^8 d_{1,i}^4 \tag{85}$$

$$\hat{E}_{1,i} = E_{1,i} + \frac{1}{2}a_{1,i}^2 \Delta t^2 \frac{1}{4}\frac{(1 - 1/2)^2}{(1 + 1/2)^2} \tag{86}$$

have been used to evaluate both the energy E and the generalized energy $\hat{E}$ of the hardening spring at the *i-th* step, which exhibits the spurious high-frequency behaviour. In Eqs. (85) and (86), $d_{1,i}$, $v_{1,i}$ and $a_{1,i}$ represent the numerical approximations of displacements, velocities and accelerations, respectively, at the instant t_i. One may observe that the time histories plotted in Fig. 11 agree with the analytical estimates (57)-(61) depicted in Fig. 4. Moreover, the capabilities of the $G - \alpha$ methods to wipe out the high-frequency components of the response and the effects of the overshoot phenomena are evident.

26

The third example deals with a *stiff* system, viz. a one-dimensional model of a clamped-free rod. Since the discontinuity in the velocity and strain (weak shocks) influences the physical solution, the high-frequency dissipation of spurious responses is a desired feature. This problem has been proposed in literature as spurious oscillations arise when non-dissipative integrators like the CAA method are adopted (Hughes and Liu (1978)). The governing equation of the problem is

$$\frac{\partial}{\partial x}\left(EA\frac{\partial u}{\partial x}\right) - \rho A\ddot{u} = 0 \tag{87}$$

with the boundary conditions

$$u\ (0,t) = 0 \text{ and } EA\frac{\partial u}{\partial x}\bigg|_{x=L} = 0. \tag{88}$$

The problem was sketched in Fig. 2a where a homogeneous elastic rod with a constant cross-sectional area was depicted. The length L of the rod is equal to 10, the density ρ and the cross sectional area A have unit values while a lumped mass matrix is used and $\mathbf{C} = \mathbf{0}$.

The system is discretized with ten elements of the same length, $L_j = \frac{L}{10} = 1$, and it has been integrated by means of the $G - \alpha$ methods with $\rho_\infty = 0.5$ and $\Delta t = 0.075$. The Young's moduli are $E_1 = 10^8$, $E_2 = 10^7$, and $E_3 = E_4 = ... = E_{10} = 10^2$. The element nodal displacement vector is defined as $\mathbf{u}_j\ (t) = [u_{j-1}\ (t), u_j\ (t)]^T$, where $u_k\ (t)$ with $k = 1, ..., 10$, is the displacement of the $k - th$ node and $u_0\ (t) = 0$ owing to the boundary conditions. Moreover, the $u_j\ (t)$, with $j = 1, ..., 10$, are the components $(\mathbf{u}\ (t))_j$ of the nodal displacement vector $\mathbf{u}\ (t)$. The mass matrix and the non-linear internal force for the $j - th$ element reads

$$\mathbf{M}_j = \frac{1}{2}A\ L_j\ \rho\ \mathbf{I}_2 \tag{89}$$

$$\mathbf{S}_j\ (\mathbf{u}_j\ (t)) = AL_jE_j\left(\mathbf{b} + \frac{4}{L_j^2}\mathbf{A}\mathbf{u}_j\ (t)\right)\varepsilon\ (\mathbf{u}_j\ (t)) \tag{90}$$

where

$$\varepsilon\ (\mathbf{u}_j\ (t)) = \mathbf{b}^T\mathbf{u}_j\ (t) + \frac{2}{L_j^2}\mathbf{u}_j^T\ (t)\ \mathbf{A}\mathbf{u}_j\ (t) \tag{91}$$

defines the scalar Green strain, $\mathbf{A} = 1/4\begin{pmatrix} 1 & -1 \\ -1 & 1 \end{pmatrix}$ and $\mathbf{b} = \frac{1}{L_j}\begin{pmatrix} -1 \\ 1 \end{pmatrix}$. In this case, Eq. (11) reads

$$\mathbf{S}_{j,\ i+1-\alpha_f}^{GEMR} = AL_jE_j\left(\mathbf{b} + \frac{4}{L_j^2}\mathbf{A}\mathbf{d}_{j,\ i+1-\alpha_f}\right)((1-\alpha_f)\varepsilon\ (\mathbf{d}_{j,\ i+1}) + \alpha_f\ \varepsilon\ (\mathbf{d}_{j,\ i})) \tag{92}$$

27

where $\mathbf{d}_{j,\,i} = [d_{j-1,\,i}, d_{j,\,i}]^T$ represents the numerical approximation of $\mathbf{u}_j\left(t_i\right)$. Again, the expressions

$$E_{1\_2,\,i} \quad = \quad \frac{1}{2}\rho A \frac{L}{10}\left(v_{1,i}^2 + v_{2,i}^2\right) + \frac{1}{2}E_1\varepsilon^2\left(\mathbf{d}_{1,\,i}\right) + \frac{1}{2}E_2\varepsilon^2\left(\mathbf{d}_{2,\,i}\right) \tag{93}$$

$$\hat{E}_{1\_2,\,i} \quad = \quad E_{1-2,\,i} + \frac{1}{2}(a_{1,i}^2 + a_{2,i}^2)\Delta t^2 \frac{1}{4}\frac{(1-1/2)^2}{(1+1/2)^2} \tag{94}$$

have been used to estimate both the energy E and the generalized energy $\hat{E}$ relevant to the high frequency components of elements 1 and 2, respectively, indicated in Fig. 2a. Moreover, $v_{k,i}$ and $a_{k,i}$ are the numerical approximation of $\dot{u}_k\left(t_i\right)$ and $\ddot{u}_k\left(t_i\right)$.

Two cases are considered in the following. In the first case, the initial conditions $(\mathbf{u}_0)_j = j/10$, $(\mathbf{v}_0)_j = \dot{u}_j\left(0\right) = 0$, for $j = 1, ..., 10$ are chosen to achieve $\mathbf{a}_0 \neq \mathbf{0}$. Due to the large elastic moduli of elements 1 and 2, see Fig. 2, only results relevant to nodes 1, 2 sensitive to the high-frequency response components and node 10 located at the rod tip are plotted. More specifically, the time histories of the displacements, velocities, accelerations, internal forces, energies and generalized energies are depicted in Fig. 12. Again, it is evident that the high-frequency components follow the analytical estimates predicted by Eqs. (57)-(61) and plotted in Fig. 4. Moreover, one may observe that such spurious components are annihilated in a few steps owing to the choice of $\rho_\infty = 0.5\ (< 1)$.

In the second case, the initial conditions $(\mathbf{u}_0)_j = 0$, $(\mathbf{v}_0)_j = -1$, for $j = 1, ..., 10$ are chosen, to achieve $\mathbf{a}_0 = \mathbf{0}$. Again, the results plotted in Fig. 13 highlight that the responses with the high-frequency components agree with the analytical estimates provided by Eqs. (57)-(61) depicted in Fig. 6.

7   Conclusions

An accuracy analysis followed by a stability analysis of the class of the $Generalized-\alpha$ methods applied to non-linear dynamical systems has been presented in this paper. It has been proved that the $G-\alpha$ methods achieve second order accuracy for displacements and velocities also in the non-linear regime, independently of the quadrature rule of the non-linear internal forces. Conversely, the computed acceleration is, in general, first order accurate. As far as the stability analysis is concerned, it has been demonstrated that the G-stability definition, suitable for linear

multistep methods applied to non-linear systems, cannot be applied to algorithms dealing with structural dynamics equations, as these equations are not contractive. Thereby, other (energy) stability definitions have been exploited, which prove that the $G - \alpha$ methods are stable in an energy sense in the high-frequency range depending on the algorithmic parameter ρ_∞. When $\rho_\infty = 0$, such algorithms are asymptotically annihilating. Conversely, the $G - \alpha$ methods entail heavy energy oscillations in the intermediate-frequency range. Moreover, the $G - \alpha$ methods have been analysed in terms of overshoot and the relevant drawbacks have been shown. Finally, results of representative numerical simulations performed on single- and multiple-degrees-of-freedom non-linear systems which exhibit key features typical of more complex systems arising in non-linear dynamics have been performed, showing the validity of the analytical estimates. The analysis of the $G - \alpha$ methods applied to forced non-linear systems subjected to potential resonant phenomena deserves additional futures studies.

8 Appendix 1. Properties of the $G - \alpha$ methods in the linear regime

In this Section, the convergence properties of the $G - \alpha$ methods in the linear regime are recalled and some links between the properties in the linear and the non-linear regime are established. Since a M.D.o.F. coupled system (3) can be decomposed into n_{DoF} uncoupled scalar equations, the analysis of the class of the $G - \alpha$ methods is performed on a S.D.o.F. model equation (Hughes (1987), p. 492). In the linear regime, Eq. (12) entails the application of the TR rule (9) and reads

$$\sum_{j=0}^{3} \left[\mathbf{M}\alpha_j \mathbf{d}_{i+j} + \Delta t \mathbf{C}\gamma_j \mathbf{d}_{i+j} + \Delta t^2 \beta_j \left(\mathbf{K}\mathbf{d}_{i+j} - \mathbf{F}_{i+j} \right) \right] = \mathbf{0} \tag{95}$$

where

$$\begin{aligned}
\beta_0 &= \alpha_f \left(\tfrac{1}{2} + \beta - \gamma \right) \\
\beta_1 &= \tfrac{1}{2} + \beta - \gamma - 3\beta\alpha_f + 2\gamma\alpha_f \\
\beta_2 &= \tfrac{1}{2} - \tfrac{\alpha_f}{2} - 2\beta + \gamma + 3\beta\alpha_f - \gamma\alpha_f \\
\beta_3 &= (1 - \alpha_f)\beta
\end{aligned} \tag{96}$$

while α_j and γ_j are defined in Eq. (13) and $\mathbf{K}$ is the symmetric positive-semidefinite stiffness matrix. Hence, Eq. (95) can be associated with the characteristic polynomial

$$\Pi(\lambda, \xi, \Omega) = \sum_{j=0}^{3} \left[\alpha_j + 2\xi\Omega\gamma_j + \Omega^2\beta_j \right] \lambda^j \tag{97}$$

where $\Omega = \omega\Delta t$, ω is the natural frequency and ξ is the damping ratio. Both the stability and accuracy properties of the $G - \alpha$ methods can be deduced through the analysis of the characteristic polynomial (97).

Given Δt, the stability of the $G - \alpha$ schemes is verified when the roots of $\Pi(\lambda, \xi, \Omega)$ are less than or equal to unity in modulus or strictly less than unity when the roots have multiplicity greater than one (Hairer and Wanner (1991), p. 256)). The conditions on the algorithmic parameters which ensure the unconditional stability of the $G - \alpha$ methods $\forall\, \Omega \in (0, \infty)$ have been derived using the Routh-Hurwitz criterion and are collected in row 2 of Table 1. The polynomial (97) admits two principal roots $\lambda_{1,2}(\xi, \Omega) = a(\xi, \Omega) + i\, b(\xi, \Omega)$ and one real spurious root λ_3. In order to maximize the high-frequency dissipation, the principal roots shall remain complex conjugate as Ω increases. Moreover, $\lim_{\Omega\to\infty} b(\xi, \Omega) = \operatorname{Im}\lambda_{1,2}^{(\infty)} = 0$ in the high-frequency limit (Chung and Hulbert (1993)). The expressions of $\lambda = \lambda(\xi, \Omega)$ for $\Omega \to \infty$ read

$$\lambda_{1,2}^{(\infty)} = \frac{4\beta - 2\gamma - 1}{4\beta} \pm \frac{i}{\beta}\sqrt{\beta - \frac{1}{4}\left(\gamma + \frac{1}{2}\right)^2}; \quad \lambda_3^{(\infty)} = \frac{\alpha_f}{-1 + \alpha_f} \tag{98}$$

and one may observe that such relations do not depend on ξ. Thereby, imposing the condition

$$\beta = \frac{1}{4}\left(\gamma + \frac{1}{2}\right)^2 \tag{99}$$

in (98) the principal roots $\lambda_{1,2}^{(\infty)}$ become real and read

$$\lambda_{1,2}^{(\infty)} = \frac{2\gamma - 3}{1 + 2\gamma} \quad \text{and} \quad \lambda_3^{(\infty)} = \frac{\alpha_f}{-1 + \alpha_f}. \tag{100}$$

The row 3 of Table 1 collects the unconditional stability conditions after imposing (99).

The condition

$$\gamma = \frac{1}{2} + \alpha_f - \alpha_m \tag{101}$$

determined in Subsection 3.1 for non-linear systems entails a second order accuracy of the $G - \alpha$ methods aside from the remaining parameters. These conditions are collected in row 4 of Table

1. The stability conditions corresponding to conditions (99) and (101) are reported in row 5 of Table 1. As a result, the class of the $G-\alpha$ methods endowed with optimal accuracy, stability and dissipation properties has two free algorithmic parameters: α_f and α_m. Setting $\alpha_f = \alpha_m = 0$ and using the condition (99) the $N-\beta$ method (Newmark (1959)) is recovered, while the CAA method requires in addition that $\gamma = \frac{1}{2}$.

The condition (101) on (100) entails

$$\lambda_{1,2}^{(\infty)} = \frac{\alpha_f - \alpha_m - 1}{\alpha_f - \alpha_m + 1} \text{ and } \lambda_3^{(\infty)} = \frac{\alpha_f}{-1 + \alpha_f}. \tag{102}$$

If $\alpha_m = 0$ and $\alpha_f = -\alpha_{HHT}$ the $HHT - \alpha$ method is retrieved (Hilber, Hughes and Taylor (1977)) while if $\alpha_m = \alpha_{WBZ}$ and $\alpha_f = 0$ the $WBZ - \alpha$ is recovered (Wood, Bossak and Zienkiewicz, (1981)). However, Chung and Hulbert (1993) enforce the condition $\lambda_3^{(\infty)} = \lambda_{1,2}^{(\infty)}$ to reduce the algorithmic damping of the $CH - \alpha$ method in the low-frequency range. Thereby, both the above-mentioned condition and (102) imply $\alpha_m = 3\alpha_f - 1$. The values of the free algorithmic parameters and the relevant relations for the $G - \alpha$ methods are summarized in Table 2.

In the low-frequency range, the condition $|\lambda_3| \leqslant |\lambda_{1,2}|$ usually holds. To avoid sharp variation of the spectral radius $\rho = \max(|\lambda_1|, |\lambda_2| |\lambda_3|)$, such inequality must hold for all $\Omega \in [0, \infty)$ (Chung and Hulbert (1993)). More specifically, the following relation

$$\left|\lambda_3^{(\infty)}\right| \leqslant \left|\lambda_{1,2}^{(\infty)}\right| \tag{103}$$

is exploited. Taking into account the relation (102), it can be shown that the condition (103) is satisfied by the $HHT - \alpha$ method if $-\frac{1}{3} \leqslant \alpha_{HHT} \leqslant 0$. The parameters of the $WBZ - \alpha$ method satisfy the condition (103) for all α_{WBZ}, while $\lambda_{1,2}^{(\infty)} = \lambda_3^{(\infty)} \forall \alpha_f$ by design in the $CH - \alpha$ method. As a result, it is convenient to set $\rho_\infty = \lim_{\Omega \to \infty} \rho(\Omega) = \left|\lambda_{1,2}^{(\infty)}\right|$ and express all the parameters as functions of ρ_∞. This single parameter $\rho_\infty \in [0, 1]$, $\rho_\infty \leqslant 1$ for the unconditional stability of the $G - \alpha$ methods and the choice $\rho_\infty = 0$ corresponds to the asymptotic annihilation of the high-frequency response, while $\rho_\infty = 1$ corresponds to the case of no algorithmic dissipation. Table 3 collects the algorithmic parameters of the $G - \alpha$ methods parametrized by ρ_∞. In all cases, $\beta = \frac{1}{(1+\rho_\infty)^2}$ and $\gamma = \frac{1}{2}\frac{3-\rho_\infty}{1+\rho_\infty}$. Moreover, $\beta \in \left[\frac{1}{4}, \frac{4}{9}\right]$ and $\gamma \in \left[\frac{1}{2}, \frac{5}{6}\right]$ for the $HHT - \alpha$ method while $\beta \in \left[\frac{1}{4}, 1\right]$ and $\gamma \in \left[\frac{1}{2}, \frac{3}{2}\right]$ for the other methods.

9   Acknowledgements

References

Abramowitz M, Stegun IA (1964) Handbook of mathematical functions. National Bureau of Standards, Appl. Math. Series 55

Bauchau OA, Damilano G, Theron NJ (1995) Numerical Integration of Non-Linear Elastic Multi-Body Systems. Int. J. for Num. Meth. in Eng. 38: 2727–2751

Belytschko T, Schoeberle DF (1975) On the unconditional stability of an implicit algorithm for non linear structural dynamics. Trans. ASME J. Appl. Mech. 42: 865–869

Chung J, Hulbert GM (1993) A time integration algorithm for structural dynamics with improved numerical dissipation: the generalized-α method. J. Appl. Mech. 60: 371–375

Crisfield MA, Galvanetto U, Jelenic G (1997) Dynamics of 3-D co-rotational beams. Comput. Mech. 20: 507–519

Crisfield MA, Shi J (1994) A co-rotational element/time-integration strategy for non-linear dynamics. Int. J. Numer. Methods Engrg. 37: 1897–1913

Hairer E, Nørsett SP, Wanner G (1987) Solving ordinary differential equations I. Springer-Verlag

Hairer E, Wanner G (1991) Solving ordinary differential equations II. Springer-Verlag

Hilber HM, Hughes TJR (1978) Collocation, dissipation and "overshoot" for time integration schemes in structural dynamics. Earthquake Engrg. Struct. Dynam. 6: 99–117

Hilber HM, Hughes TJR, Taylor RL (1977) Improved numerical dissipation for time integration algorithms in structural dynamics. Earthquake Engrg. Struct. Dynam. 5: 283–292

Hoff C, Pahl PJ (1988a) Development of an implicit method with numerical dissipation from a generalized single-step algorithm for structural dynamics. Comput. Methods Appl. Mech. Engrg. 67: 367–385

Hoff C, Pahl PJ (1988b) Practical performance of θ_1 -method and comparison with other dissipative algorithms in structural dynamics. Comput. Methods Appl. Mech. Engrg. 67: 87–110

Houbolt JC (1950) A recurrence matrix solution for the dynamic response of elastic aircraft. J. Aeronaut. Sci. 17: 540–550

Hughes TJR (1975) A note on the stability of Newmark's algorithm in nonlinear structural dynamics

Hughes TJR (1976) Stability, convergence and growth and decay of energy of the average acceleration method in nonlinear structural dynamics. Comput. & Struct. 6: 313–324

Hughes TJR (1987) The finite element method, linear static and dynamic finite element analysis. Prentice-Hall

Hughes TJR, Liu WK (1978) Implicit-Explicit Finite Elements in Transient Analysis: Implementation and Numerical Examples. J. Appl. Mech. (60): 371–375

Hulbert GM (1991) Limitations on linear multistep method for structural dynamics. Earthquake Engrg. Struct. Dynam. 20: 191–196

Hulbert GM, Hughes TJR (1987) An error analysis of truncated starting conditions in step-by-step time integration: consequences for structural dynamics. Earthquake Engrg. Struct. Dynam. 15: 901–910

Hulbert GM, Jang I (1995) Automatic Time Step Control Algorithms for Structural Dynamics. Comp. Methods Appl. Mech. Eng. 126: 155–178

Karabalis DL, Beskos DE (1997) Numerical methods in earthquake engineering in Computer analysis and design of earthquake resistant structures. A handbook. Computational Mechanics Publications

Kuhl D, Crisfield MA (1999) Energy Conserving and Decaying Algorithms in Non-Linear Structural Dynamics. Int. J. Numer. Methods Engrg. 45: 569–599

Kuhl D, Ramm E (1996) Constraint Energy Momentum alghorithm and its application to non-linear dynamics of shells. Comput. Methods Appl. Mech. Engrg.

Kuhl D, Ramm E (1999) Generalized Energy-Momentum Method for non-Linear adaptive shell dynamics. Comput. Methods Appl. Mech. Engrg. 178: 343–366

Lambert JD (1991) Numerical methods for ordinary differential systems. John Wiley & Sons

Newmark NM (1959) A method of computation for structural dynamics. J. Engrg. Mech. Div. ASCE 85(EM3): 67–94

Owren B, Simonsen HH (1995) Alternative Integration Methods for Problems in Structural Dynamics. Comput. Methods Appl. Mech. Engrg. 122: 1–10

Park KC (1975) An improved stiffy stable method for direct integration of nonlinear structural dynamic equations. Trans. ASME J. Appl. Mech. 42: 464–470

Simo JC, Tarnow N (1992) The Discrete Energy-Momentum Method. Conserving Algorithms for Nonlinear Elastodynamics. Z. angew. Math. Phys 43: 757–792

Stuart AM, Humphries AR (1996) Dynamical systems and numerical analysis. Cambridge University Press

Tamma KK, Zhou X, Sha D (2000) The time dimension: A theory towards the evolution, classification, characterization and design of computational algorithms for transient/dynamic applications. Archives of Comput. Methods in Engrg. 7: 67–290

Wood WL (1990) Pratical time-stepping schemes. Oxford University Press

Wood WL, Bossak M, Zienkiewicz OC (1981) An alpha modification of Newmark's method. Int. J. Numer. Methods Engrg. 15: 1562–1566

Wood WL, Oduor ME (1988) Stability properties of some algorithms for the solution of nonlinear dynamics vibration equations. Comm. Appl. Numer. Methods 4: 205–212

Zhong HG, Crisfield MA (1998) An Energy-Conserving Co-Rotational Procedure for the Dynamics of Shell Structures. Engng. Comput. 15(5): 552–576

10 List of Tables

Table 1. Unconditional stability conditions for the algorithmic parameters of the $G - \alpha$ methods. S: Stability; O.D.: Optimal Dissipation; S.O.A.: Second Order Accuracy.

Table 2. Relations among the algorithmic parameters in order to achieve first order accuracy for the $N - \beta$ method, second order accuracy for the $\alpha-$ methods and corresponding unconditional stability conditions.

Table 3. Relations among the algorithmic parameters of the $N - \beta$ and the $\alpha-$ methods expressed as functions of the spectral radius ρ_∞ and corresponding ranges.

11   List of Figures

Fig. 13. Evolution of acceleration, velocity, displacement, reaction force, energy and generalized energy for a non-linear clamped-free homogeneous elastic rod with $\mathbf{a}_0 = \mathbf{0}$, $\mathbf{C} = \mathbf{0}$, $\rho_\infty = 0.5$, $\mathbf{u}_0 = \mathbf{0}$, $(\mathbf{v}_0)_j = $ -1 and $\Delta t = 0.075$.

Parameter conditions	α_m	α_f	β	γ
S	$\frac{1}{2} - (\gamma - \alpha_f) \leqslant \alpha_m \leqslant \frac{1}{2}$	$\leqslant \frac{1}{2}$	$\geqslant \frac{\gamma}{2}$	$\geqslant \frac{1}{2}$
S and O.D. (99)	$\frac{1}{2} - (\gamma - \alpha_f) \leqslant \alpha_m \leqslant \frac{1}{2}$	$\leqslant \frac{1}{2}$	$\frac{1}{4}\left(\gamma + \frac{1}{2}\right)^2$	$\geqslant \frac{1}{2}$
S and S.O.A. (101)	$\leqslant \alpha_f$	$\leqslant \frac{1}{2}$	$\geqslant \frac{1}{4} + \frac{1}{2}(\alpha_f - \alpha_m)$	$\frac{1}{2} + \alpha_f - \alpha_m$
S, (99) and (101)	$\leqslant \alpha_f$	$\leqslant \frac{1}{2}$	$\frac{1}{4}\left(1 + \alpha_f - \alpha_m\right)^2$	$\frac{1}{2} + \alpha_f - \alpha_m$

Table 1. Unconditional stability conditions for the algorithmic parameters of the $G - \alpha$ methods. S: Stability; O.D.: Optimal Dissipation; S.O.A.: Second Order Accuracy.

Method	α_m	α_f	β	γ
$N - \beta$	0	0	$\frac{1}{4}\left(\gamma + \frac{1}{2}\right)^2$	$\geqslant \frac{1}{2}$
$HHT - \alpha$	0	$0 \leqslant -\alpha_{HHT} \leqslant \frac{1}{2}$	$\frac{1}{4}\left(1 - \alpha_{HHT}\right)^2$	$\frac{1}{2} - \alpha_{HHT}$
$WBZ - \alpha$	$\alpha_{WBZ} \leqslant 0$	0	$\frac{1}{4}\left(1 - \alpha_{WBZ}\right)^2$	$\frac{1}{2} - \alpha_{WBZ}$
$CH - \alpha$	$3\alpha_f - 1$	$\leqslant \frac{1}{2}$	$\left(1 - \alpha_f\right)^2$	$\frac{3}{2} - 2\alpha_f$

Table 2. Relations among the algorithmic parameters in order to achieve first order accuracy for the $N - \beta$ method, second-order accuracy for the $\alpha-$ methods and corresponding unconditional stability conditions.

Method	ρ_∞	α_m	α_f
$N - \beta$	$-\frac{2\gamma - 3}{1 + 2\gamma} \in [0, 1]$	0	0
$HHT - \alpha$	$\frac{1 + \alpha_{HHT}}{1 - \alpha_{HHT}} \in \left[\frac{1}{2}, 1\right]$	0	$-\alpha_{HHT} = \frac{1 - \rho_\infty}{1 + \rho_\infty} \in \left[0, \frac{1}{3}\right]$
$WBZ - \alpha$	$\frac{1 + \alpha_{WBZ}}{1 - \alpha_{WBZ}} \in [0, 1]$	$\alpha_{WBZ} = \frac{\rho_\infty - 1}{1 + \rho_\infty} \in [-1, 0]$	0
$CH - \alpha$	$\frac{\alpha_f}{1 - \alpha_f} \in [0, 1]$	$\frac{2\rho_\infty - 1}{1 + \rho_\infty} \in \left[-1, \frac{1}{2}\right]$	$\frac{\rho_\infty}{1 + \rho_\infty} \in \left[0, \frac{1}{2}\right]$

Table 3. Relations among the algorithmic parameters of the $N - \beta$ and the $\alpha-$ methods expressed as functions of the spectral radius ρ_∞ and corresponding ranges.
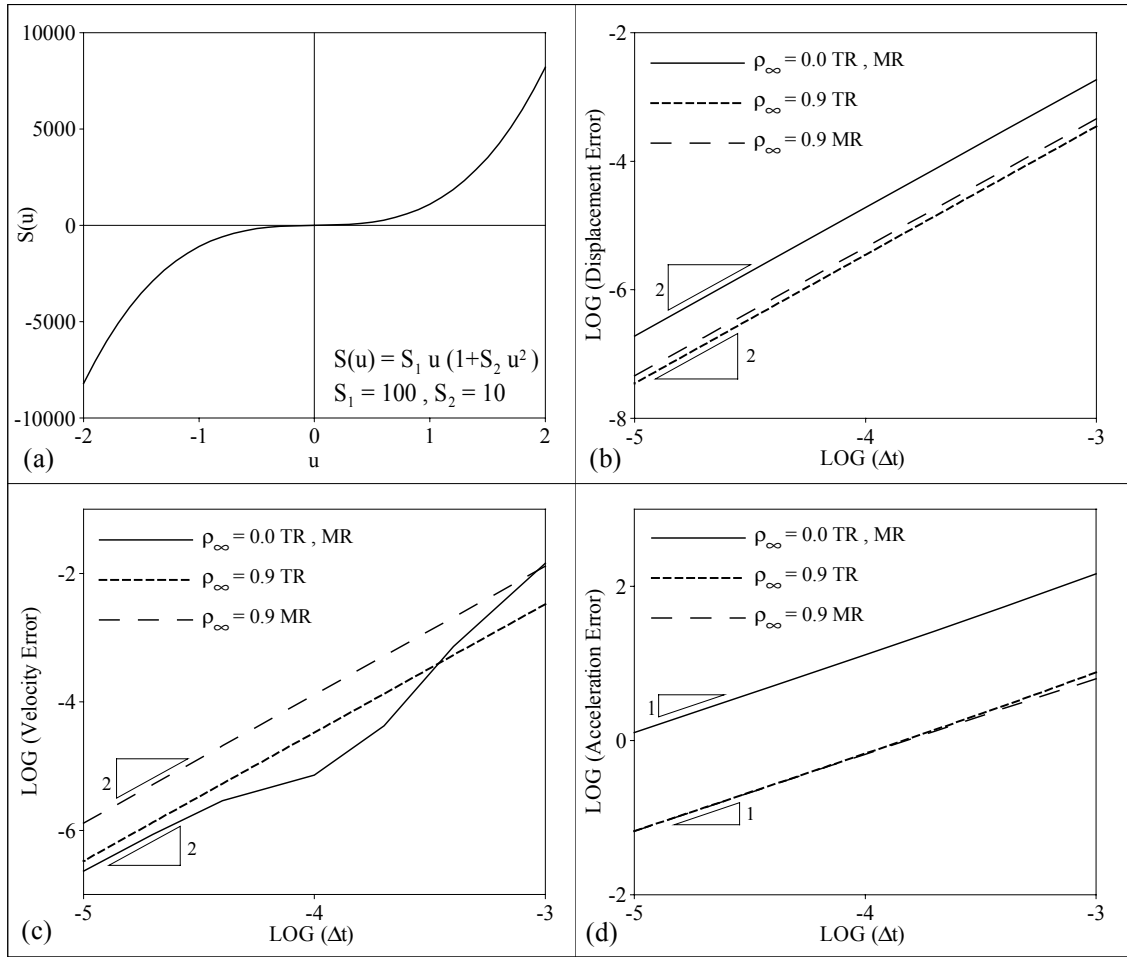
Fig. 1. **a** Reaction force vs. displacement of an undamped Duffing hardening oscillator; **b** convergence of displacement at t = 0.02 with u_0 = 1.5, v_0 = 0; **c** convergence of velocity at t = 0.02; **d** convergence of acceleration at t = 0.02 .
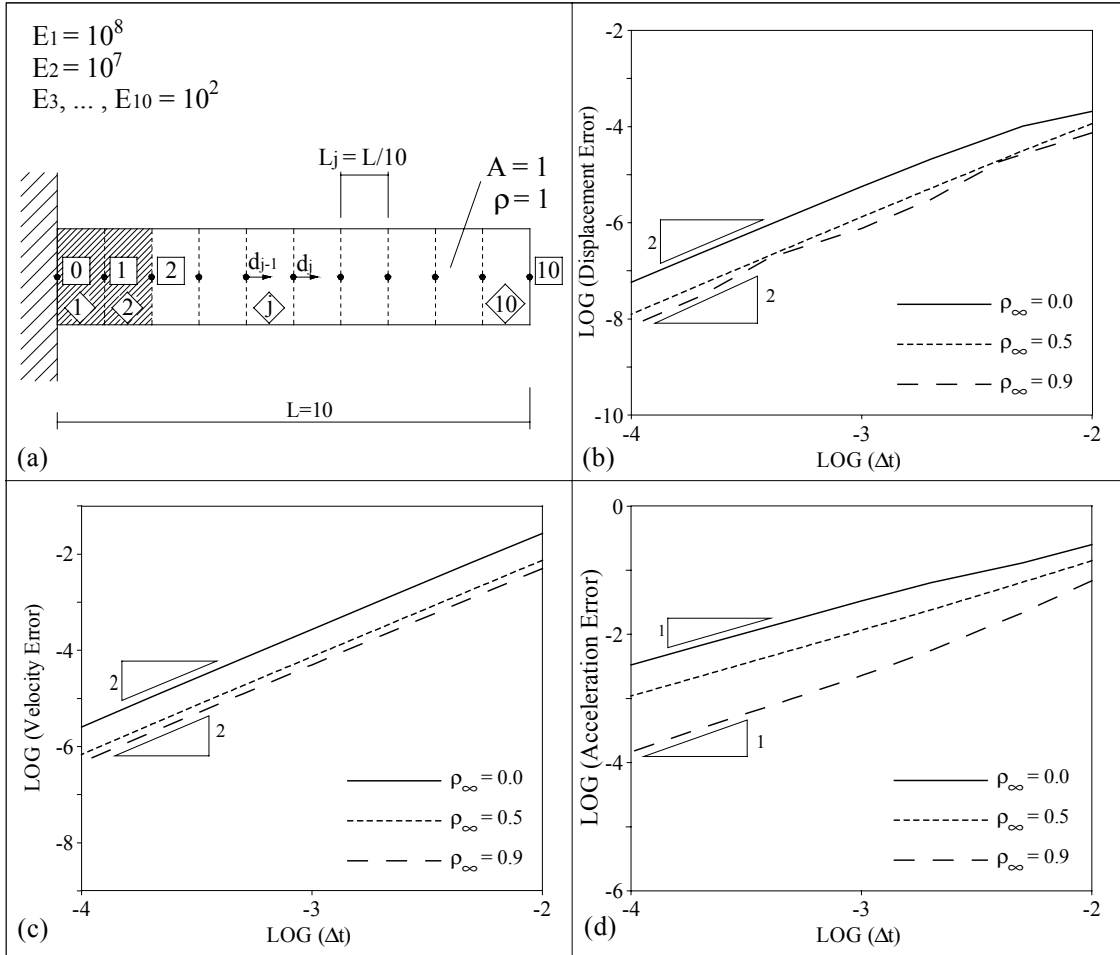
Fig. 2. **a** Non-linear undamped clamped-free homogeneous elastic rod with a constant cross-sectional area; **b** convergence of displacement at t = 0.2 with $(\mathbf{u}_0)_j = j / 10$, $\mathbf{v}_0 = \mathbf{0}$; **c** convergence of velocity at t = 0.2; **d** convergence of acceleration at t = 0.2 .
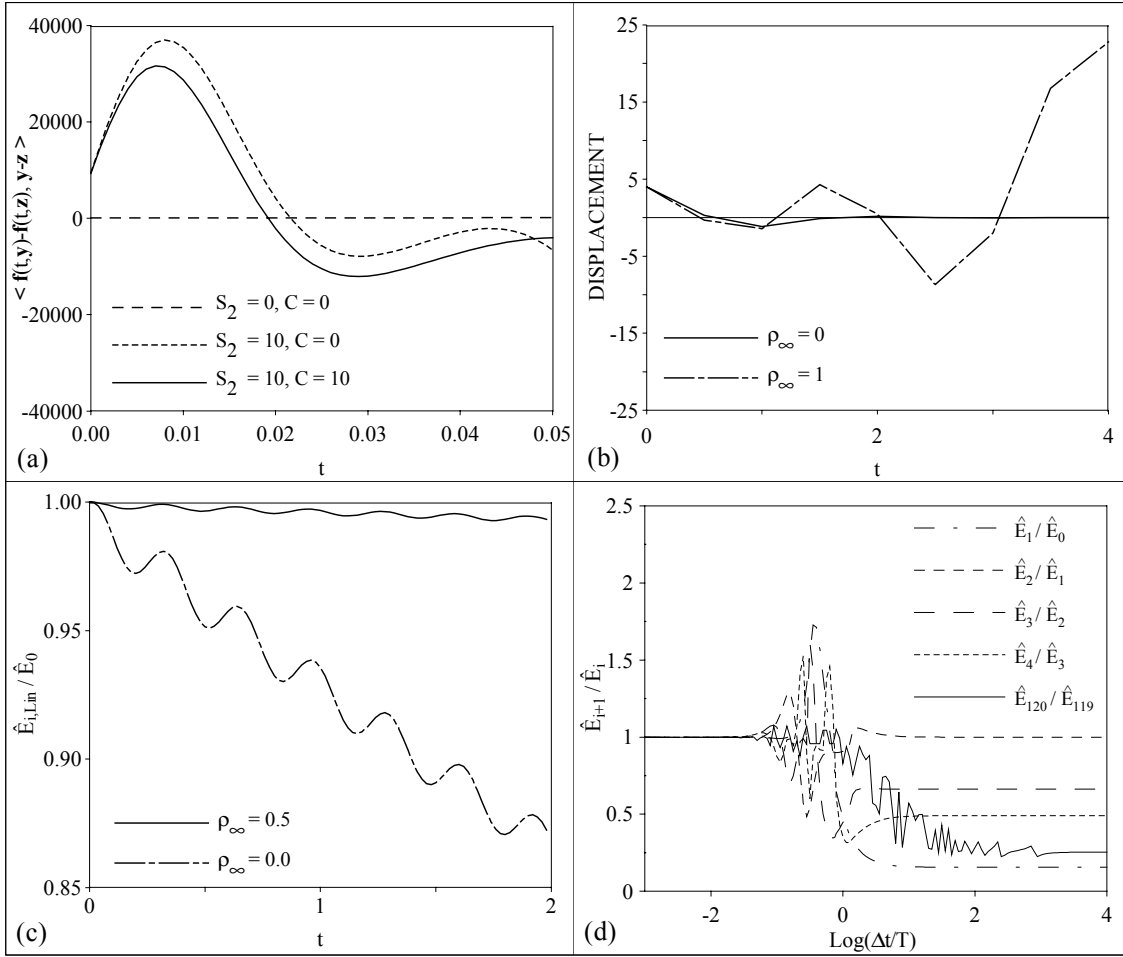
Fig. 3. **a** Evolution of $< \mathbf{f}(t,\mathbf{y}) - \mathbf{f}(t,\mathbf{z}) , \mathbf{y} - \mathbf{z} >$ for a Duffing hardening oscillator with different parameters and $\mathbf{y}_0^T$ = $(u_{y_0} , v_{y_0}) = (1.5, 1)$, $\mathbf{z}_0^T = (u_{z_0} , v_{z_0}) = (1, 5)$ and $\Delta t = 0.001$; **b** Evolution of the undamped softening oscillator with $u_0 = 4$, $v_0 = 0$ and $\Delta t = 0.5$; **c** Evolution of the energy norm ratio for a linear undamped system with natural frequency $\omega = 10$, $u_0 = 1.5$, $v_0 = 0$ and $\Delta t/T = 1/(10\pi)$; **d** Energy norm ratios for an undamped Duffing hardening oscillator with $u_0 = 1.5$ and $v_0 = 0$.
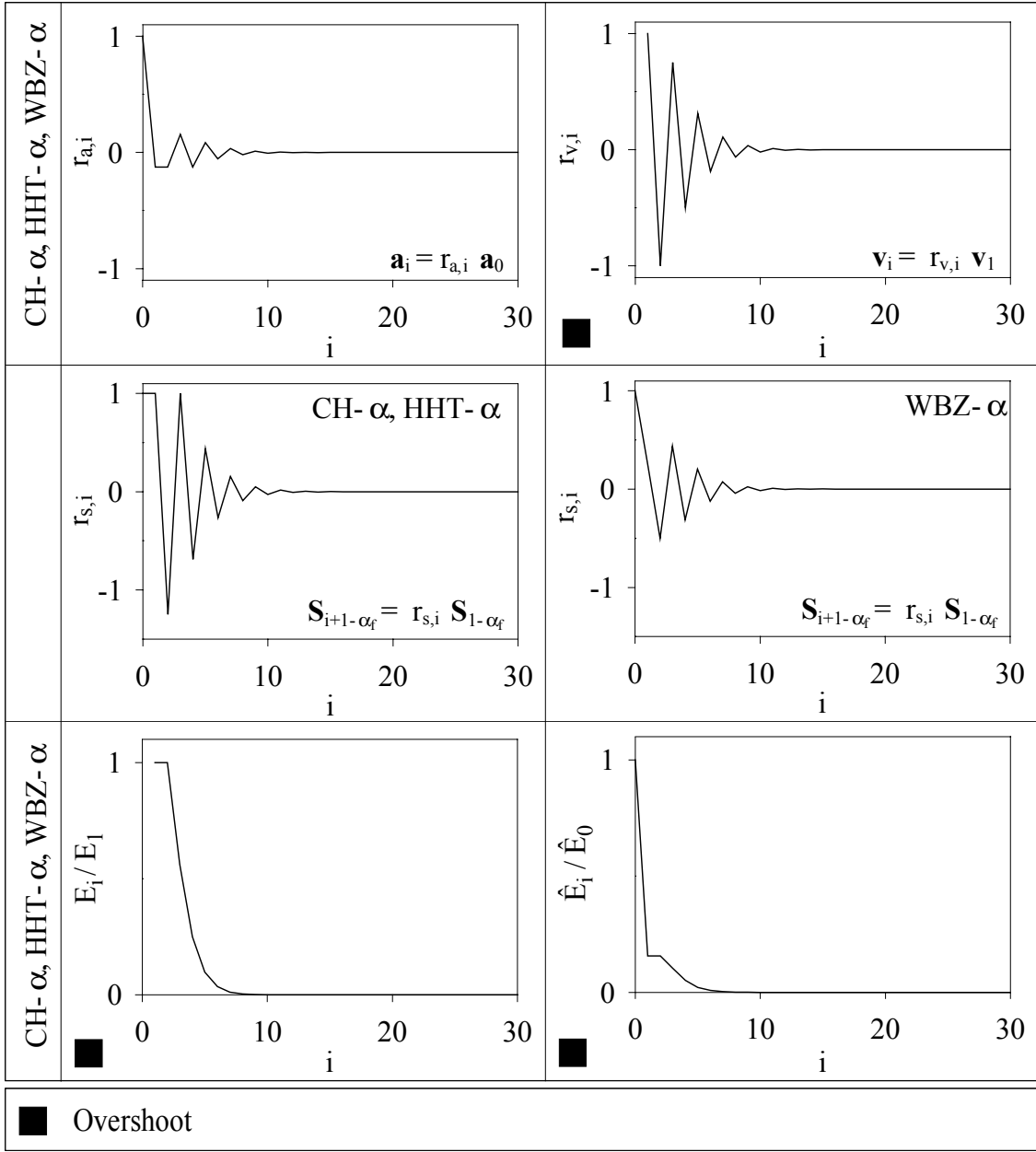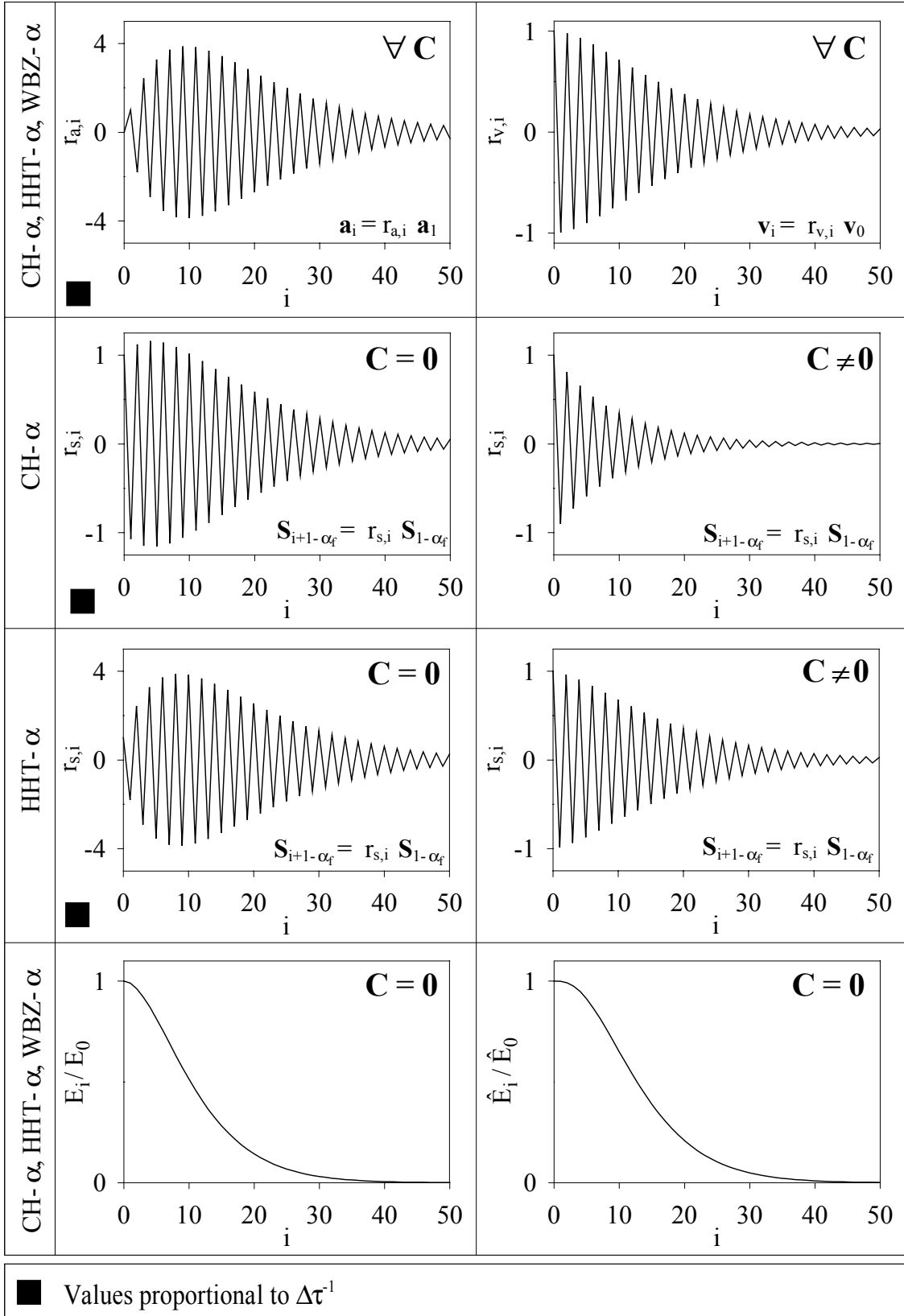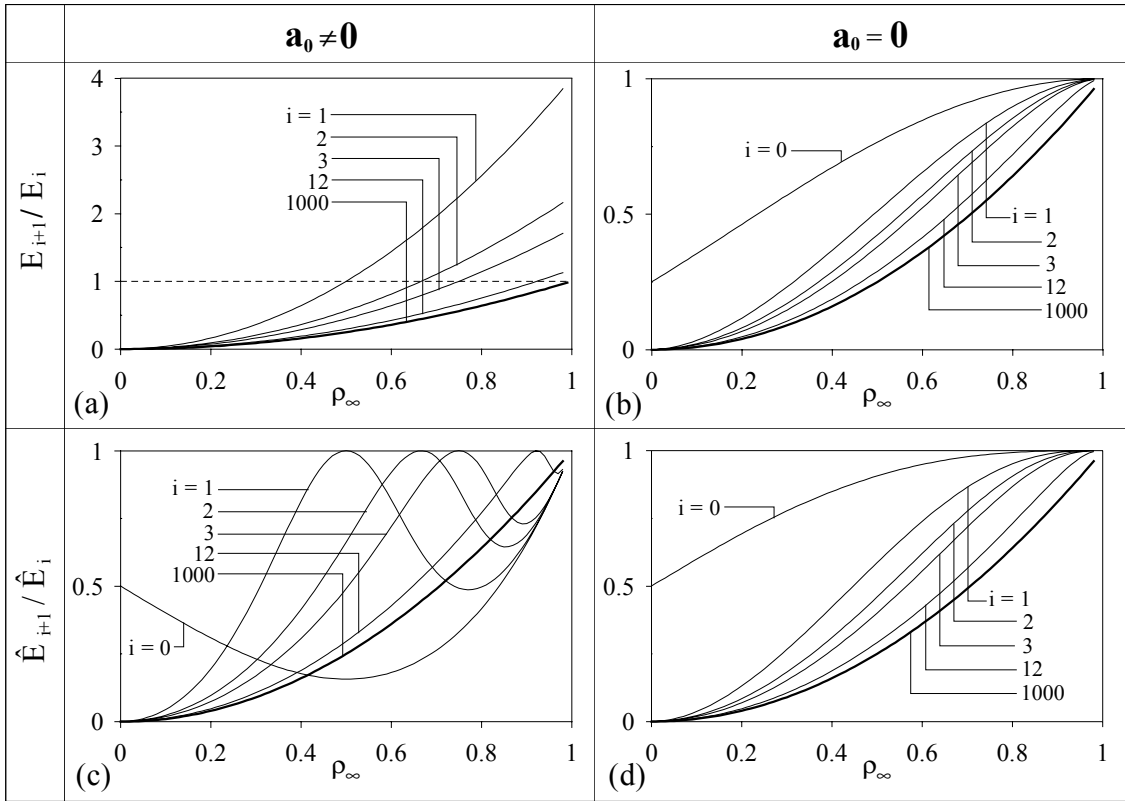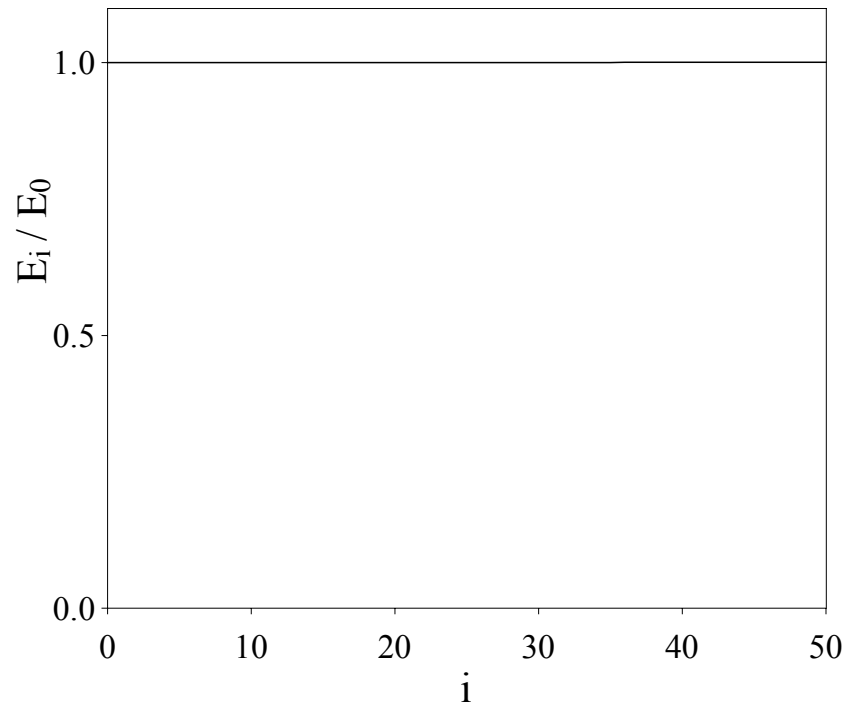
Fig. 4. Evolution of the ratios of acceleration, velocity, reaction force, energy and generalized energy for $\mathbf{a_0} \neq \mathbf{0}$, $\mathbf{C} = \mathbf{0}$, $\rho_\infty = 0.5$ and $\Delta\tau \gg 1$.
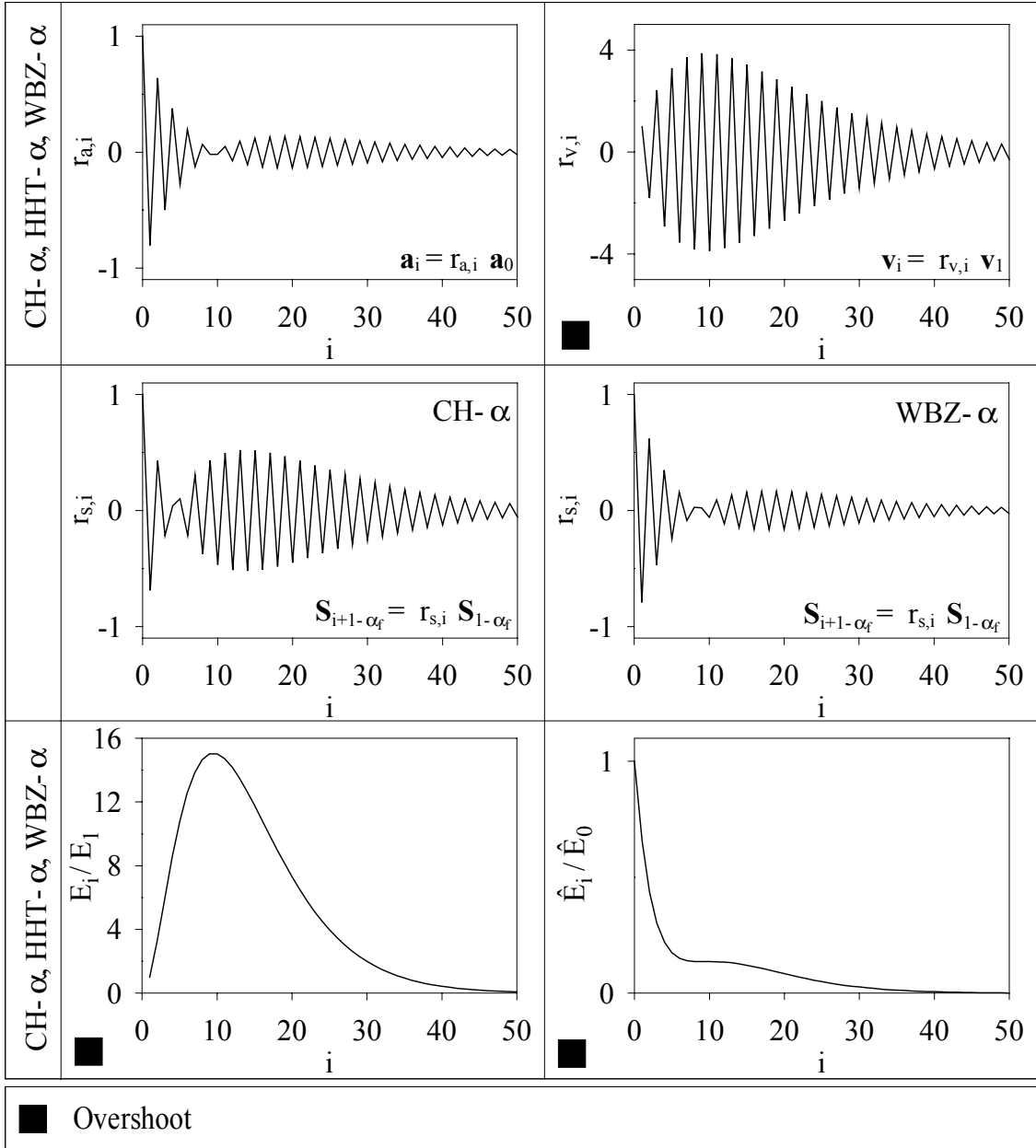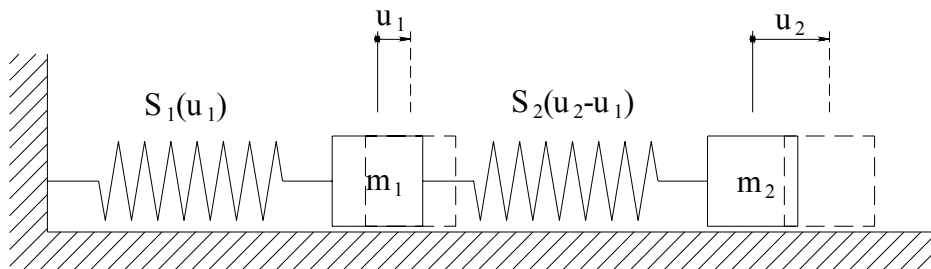
Fig. 5. Evolution of the ratios of acceleration, velocity, reaction force, energy and generalized energy for $\mathbf{a_0} \neq \mathbf{0}$, $\mathbf{C} = \mathbf{0}$, $\rho_\infty = 0.9$ and $\Delta\tau \gg 1$.
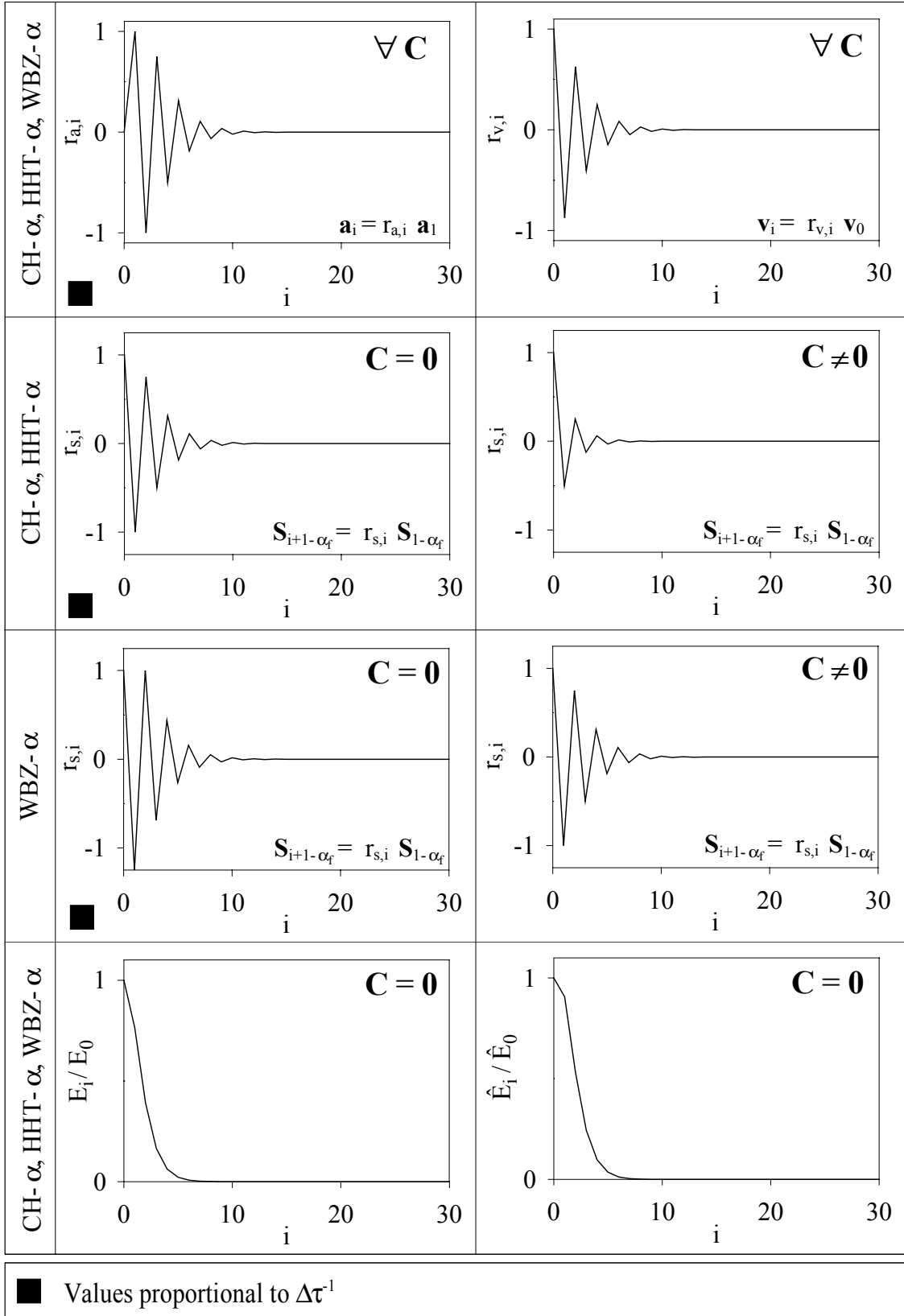
Fig. 6. Evolution of the ratios of acceleration, velocity, reaction force, energy and generalized energy for $\mathbf{a}_0 = \mathbf{0}$, $\rho_\infty = 0.5$ and $\Delta\tau \gg 1$.
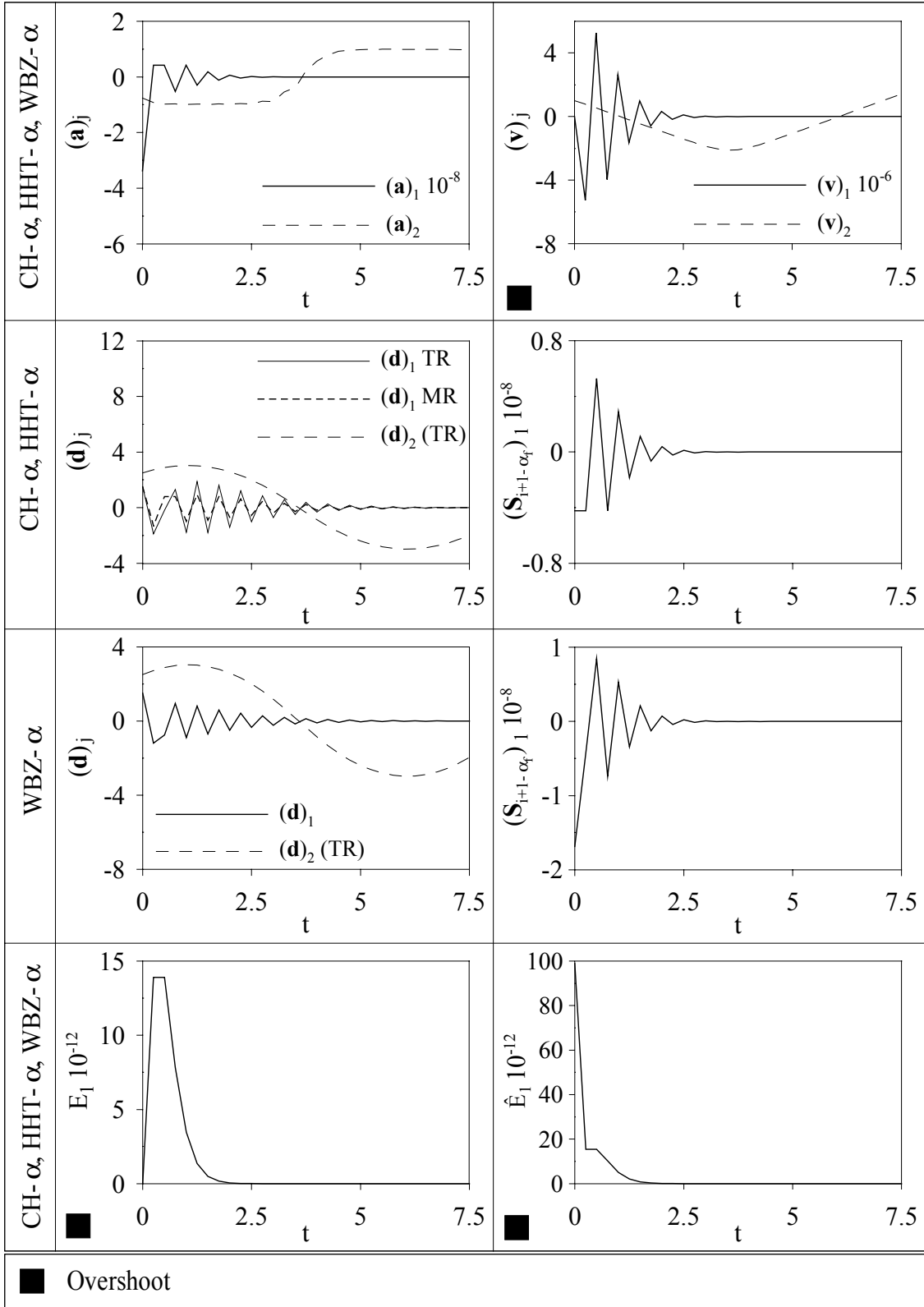
Fig. 7. Evolution of the ratios of acceleration, velocity, reaction force, energy and generalized energy for $\mathbf{a_0} = \mathbf{0}$, $\rho_\infty = 0.9$ and $\Delta\tau \gg 1$.

Values proportional to $\Delta\tau^{-1}$

Fig. 8. Evolution of the ratios of energy and generalized energy for $\mathbf{C = 0}$ and $\Delta\tau \gg 1$.

Fig. 9. Evolution of the energy ratio E_i / E_0 for an undamped Duffing hardening oscillator with $u_0 = 1.5$, $v_0 = 0$ and $\Delta T = 151,53$.

Fig. 10. Non linear two D.o.F. system

Fig. 11. Evolution of acceleration, velocity, reaction force, energy and generalized energy for a non-linear two D.o.F. system with $\mathbf{a_0} \neq \mathbf{0}$, $\mathbf{C} = \mathbf{0}$, $\rho_\infty = 0.5$, $\mathbf{u_0}^T = \{1.5, 2.5\}$, $\mathbf{v_0}^T = \{0, 1\}$ and $\Delta t = 0.25$.
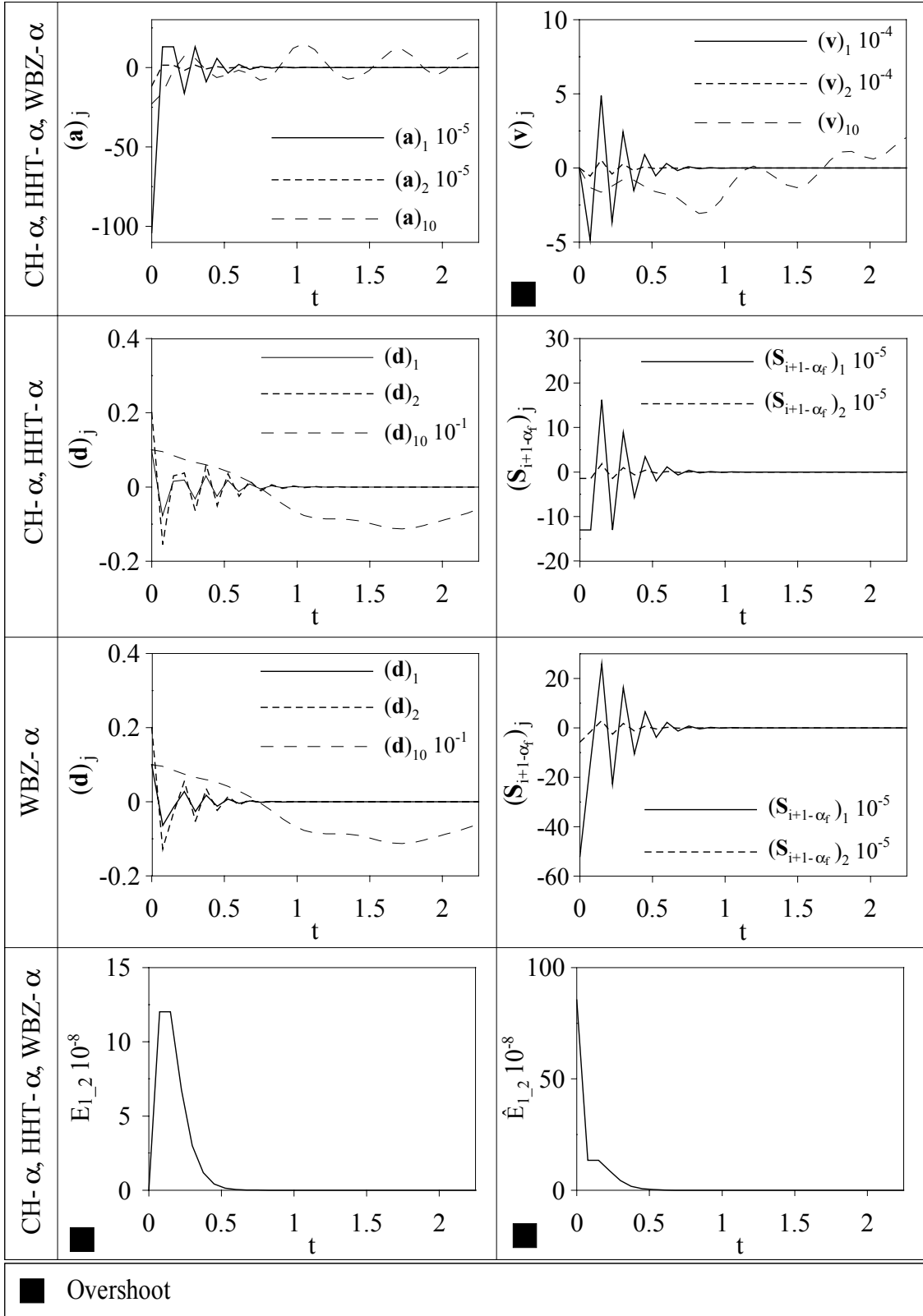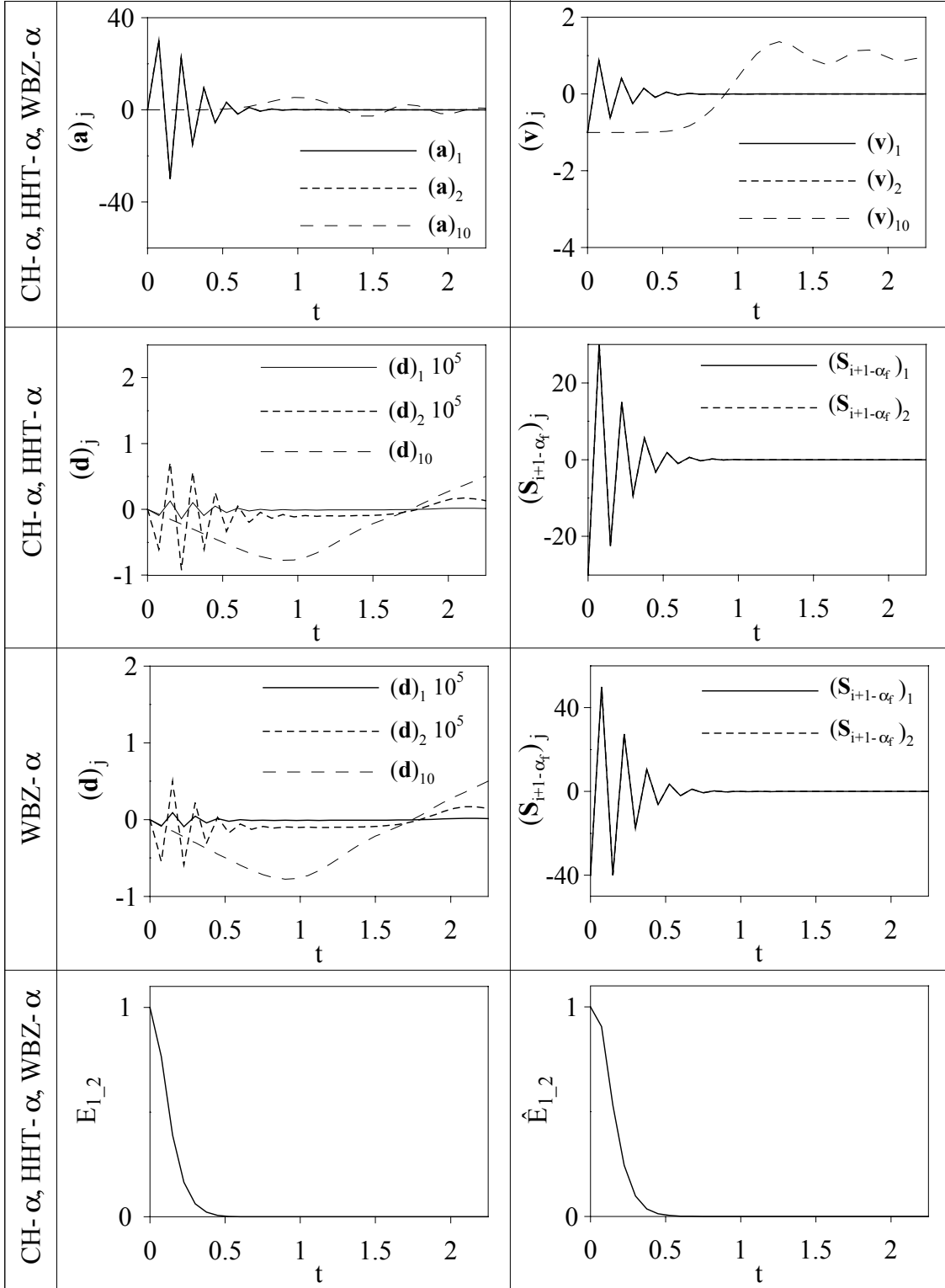
47

Fig. 12. Evolution of acceleration, velocity, reaction force, energy and generalized energy for a non-linear clamped-free homogeneous elastic rod with $\mathbf{a_0} \neq \mathbf{0}$, $\mathbf{C} = \mathbf{0}$, $\rho_\infty = 0.5$, $(\mathbf{u_0})_j = j/10$, $\mathbf{v_0} = \mathbf{0}$ and $\Delta t = 0.075$.

Fig. 13. Evolution of acceleration, velocity, reaction force, energy and generalized energy for a non-linear clamped-free homogeneous elastic rod with $\mathbf{a_0} = \mathbf{0}$, $\mathbf{C} = \mathbf{0}$, $\rho_\infty = 0.5$, $\mathbf{u_0} = \mathbf{0}$, $(\mathbf{v_0})_j = -1$ and $\Delta t = 0.075$.